Micro-mechanically guided high-throughput alloy design exploration towards metastability-induced H embrittlement resistance

**PI: C. Cem Taşan, Ju Li, Bilge Yildiz (MIT),
Joost J. Vlassak (Harvard)**

DOE project Award No.: DE-EE0008830

June 6-8, 2022

Massachusetts Institute of Technology

Project Goal

- Develop a novel high-throughput compositional and microstructural screening approach to design new alloys with superior hydrogen embrittlement (HE)-resistance, by specifically focusing on the use of metastability effects on toughening. This includes:

  (i) Technique development of high-throughput screening (HTS) for HE-resistance

  (ii) Discovery of new metallic materials with superior HE-resistance using the HTS techniques

  (iii) Multiscale verification of HE-resistance of the new alloys and H-barrier layers, from atomic scale to an engineering scale

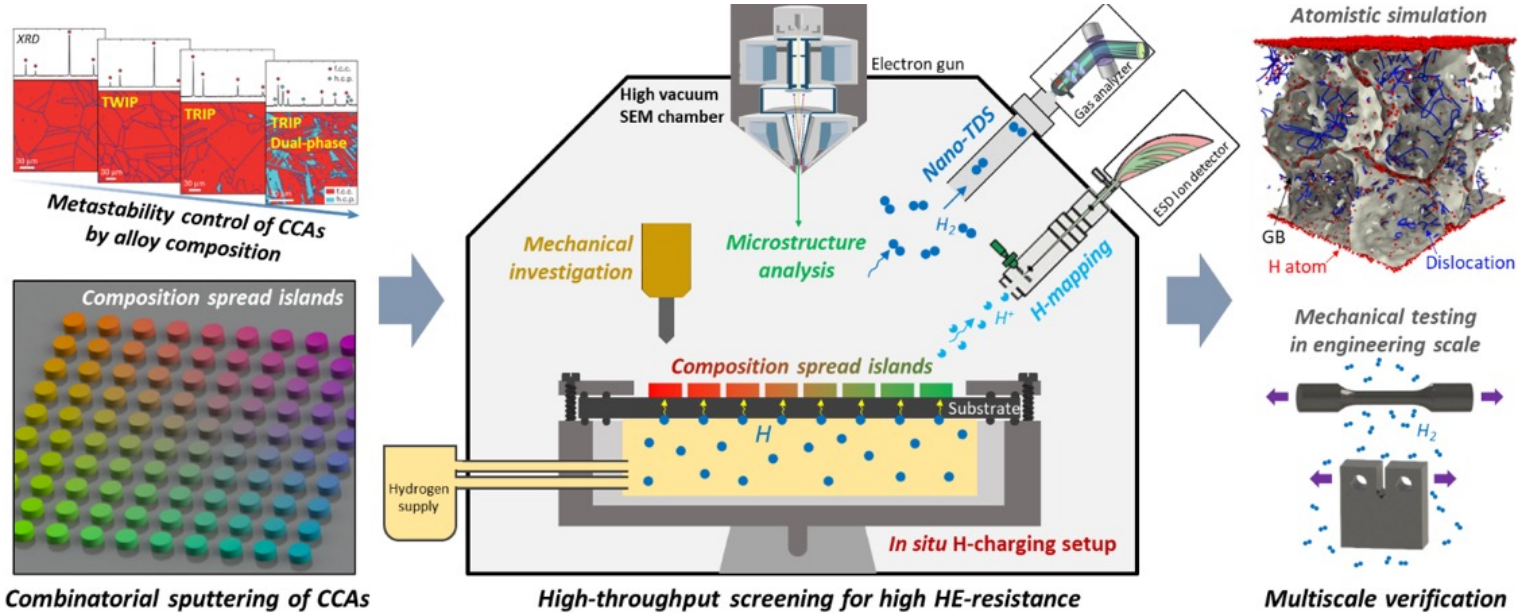

Overview

TBU

Timeline

- Project Start Date: 04/01/20
- Project End Date: 03/31/23

Barriers

- Key barriers addressed in the project are:
  - Hydrogen delivery, E. Gaseous Hydrogen Storage and Tube Trailer Delivery Costs
  - Hydrogen storage, G. Materials of construction

Budget

- Total Project Budget: $1,250,000
- Total DOE Share: $1,000,000
- Total Cost Share: $250,000
- Total DOE Funds Spent*: $681,921.62
- Total Cost Share Funds Spent*: $214,629.16

*Estimated as of 03/31/22

Partners

- Project lead: C. Cem Tasan (MIT)
- Co-PIs: Ju Li, Bilge Yildiz (MIT), Joost J. Vlassak (Harvard)
- Partner organization: ATI

Taşan Group

Relevance

Objectives:

- Develop a novel rapid alloy design methodology for high HE-resistance, integrating micromechanical screening of composition spread island films and multi-scale verification by bulk alloy testing and atomistic simulation. The outcome can significantly accelerate new metallic material exploration process and screening of HE-resistance, which rare equired for “Safe, Lower Cost Containment Technologies” in HFTO MYRDD.
- Explore a complex-concentrated alloy (CCA) space in which phase metastability (related to deformation-induced phase transformation and mechanical twinning) can be utilized to enhance HE-resistance, using a new high-throughput alloy design methodology.

Barrier from HFTO MYRDD	Impact from this project
Hydrogen delivery, E. Gaseous Hydrogen Storage and Tube Trailer Delivery Costs	Provide novel methods to drastically reduce the required R&D period for new alloy development as well as H-related physical property screening of multiple alloys
Hydrogen storage, G. Materials of construction	

Approach: *Integrated high-throughput alloy design strategy*

Metastability control of Complex-Concentrated Alloys (CCAs) by composition

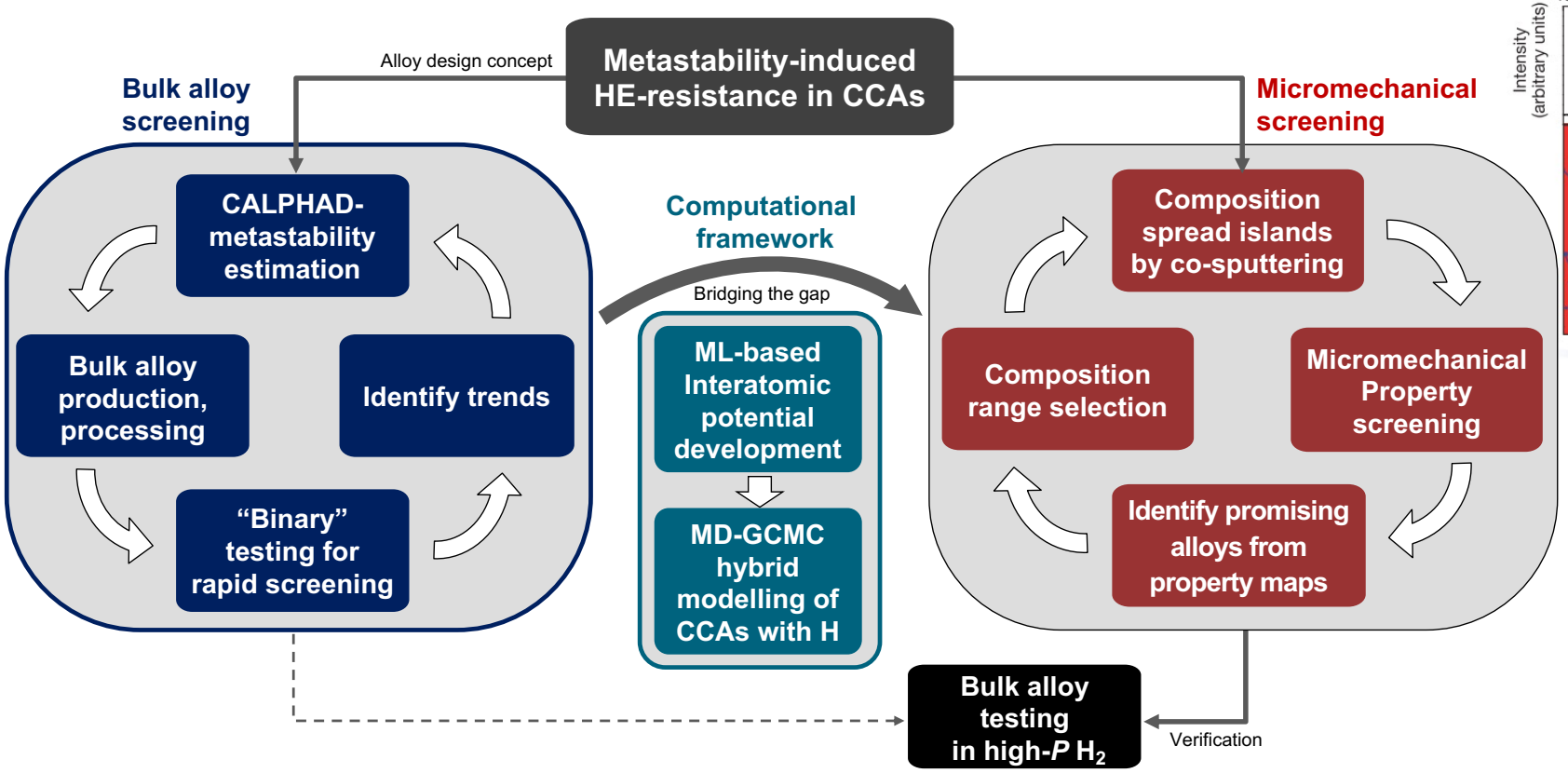

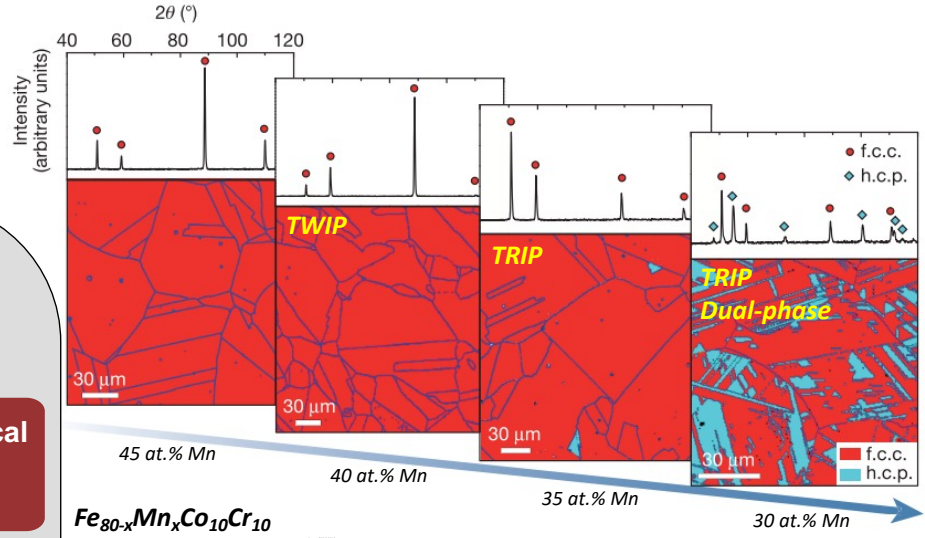

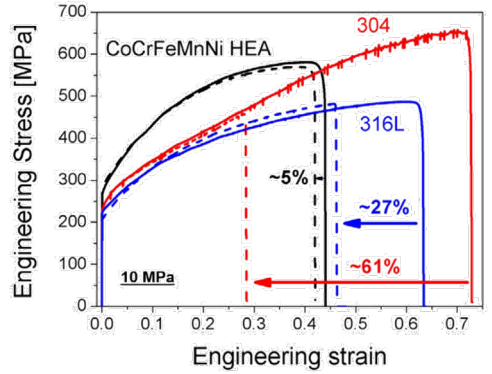

Key focus: Enhance HE-resistance by controlling phase metastability that induces plasticity mechanism transition, and which can be manipulated by composition optimization of CCAs.

Approach: *CALPHAD-based bulk alloy high-throughput screening*

CALPHAD-informed composition selection → **Alloy production, Thermomechanical processing** → **"Binary" testing: Go/no-Go decision** → **Evaluate results, Identify trends**

- Key focus: maximizing range of microstructures
  - Cast a small number of compositions, post-process to vary microstructures
- Adapted from other alloy design routes:
  - Rapid alloy prototyping
  - Iterative approaches based on machine learning
- Goal: explore HE dependence on phase constitution & transformations in CCAs
  & provide composition ranges to be explored by micromechanical approach in detail

Approach: *Micromechanics-based high-throughput screening*

Bulk alloy testing -informed composition range selection → **Fabrication of composition spreads (Composition library)** → **Rapid property screening with *in situ* H-charging** → **Identify trends from property maps, Verify in bulk scale**

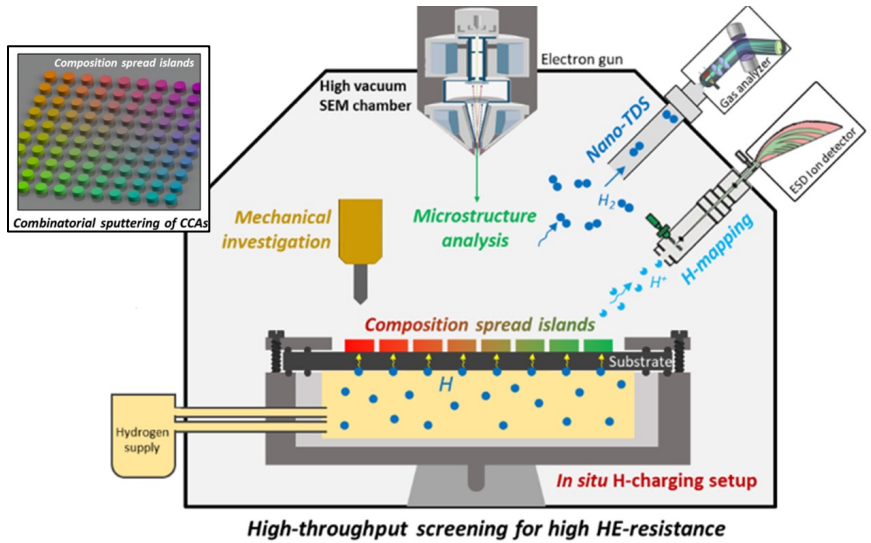

High-throughput screening for high HE-resistance

- Key focus: Rapid property screening on composition spreads
- Property mapping using micromechanical tests
  - *In situ* H-charging indentation-based approach
  - Metastability mapping by H & stress-induced change
- Goal: explore H & deformation-induced microstructural change depending on alloy compositions and phase metastability

Approach: *Computational framework for complex alloys*

Workflow of multicomponent interatomic potential development

Deep-potential generator (DP-Gen): concurrent learning scheme

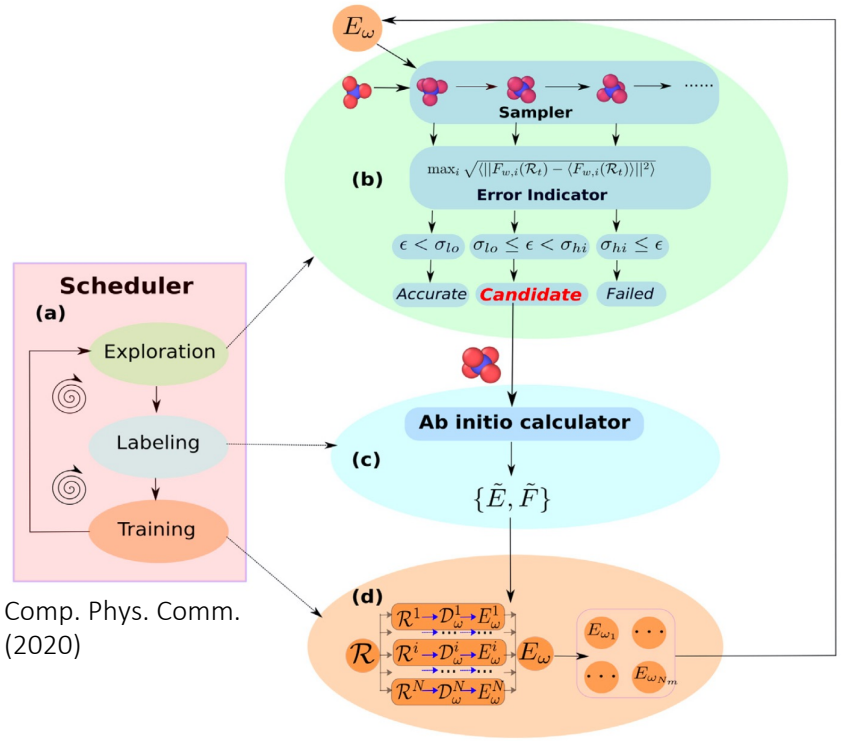

Comp. Phys. Comm. (2020)

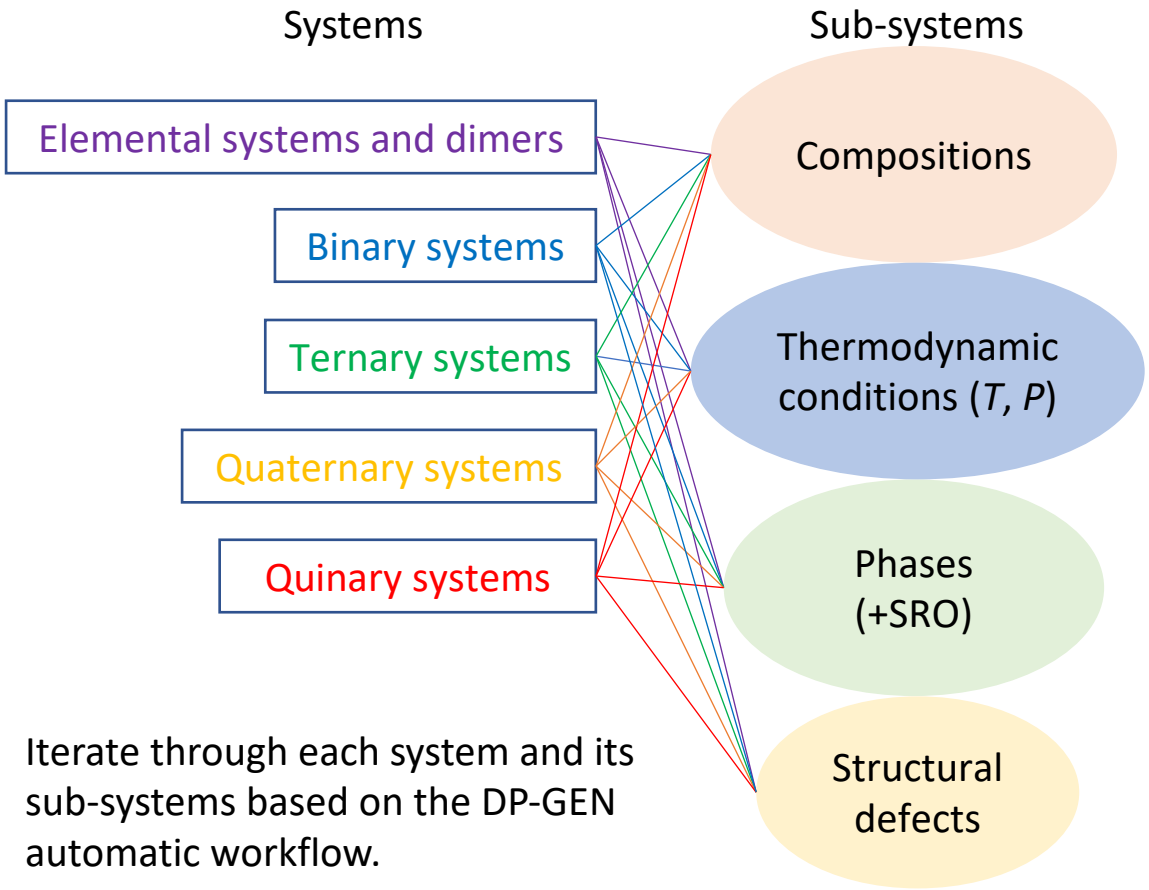

Iterate through each system and its sub-systems based on the DP-GEN automatic workflow.

- Key focus: Establish computational framework for exploring complex multicomponent alloys
- Goal: Bridging the gap between bulk and microscale studies, mainly induced by defect structures

Brief Summary of Past Results

CALPHAD-informed bulk alloy screening

CALPHAD: Austenite stability estimation

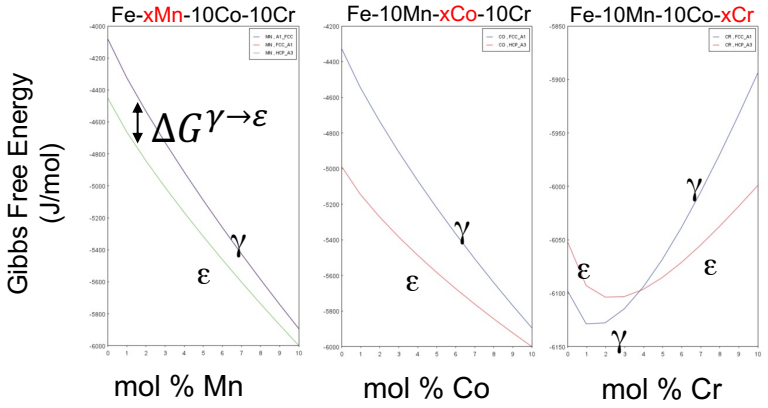

Alloy selection and production

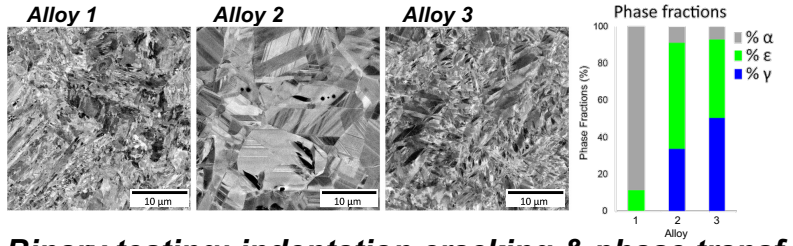

Binary testing: indentation cracking & phase transf.

	Pre-H Indentation		Post-H Indentation		Post-Outgassing Indent.	
Alloy	α' transf?	Cracking?	α' transf?	Cracking?	α' transf?	Cracking?
2	Y	N	Y	N	Y	N
3	Y	N	N	Y	N	Y

ML-based Simulations

Workflow of multicomponent interatomic potential development

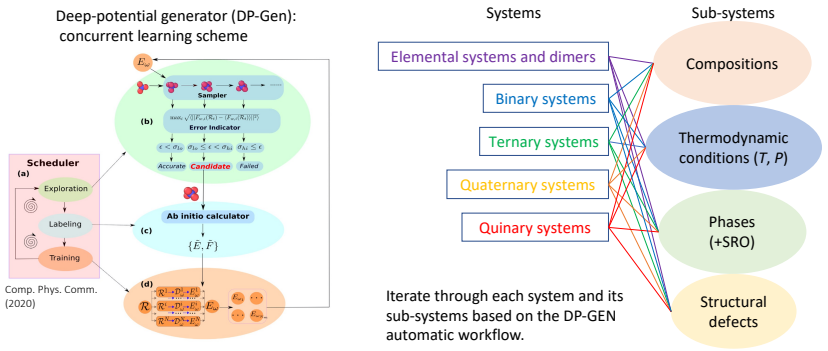

GCMC-MD simulation of H in binary alloy – effect of grain boundary orientation

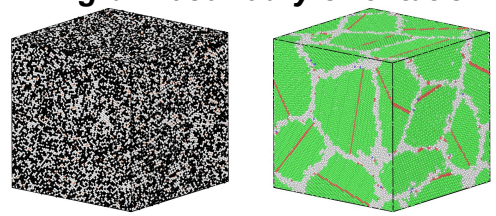

- 50% Ni (white) + 50% Al (black)
Hydrogen (Red): c_H = 4.8%

- Green: FCC atoms
Red: Twin boundaries
Grey: Random grain boundaries

- Polycrystal under H-charging μ_H = -2.25 eV

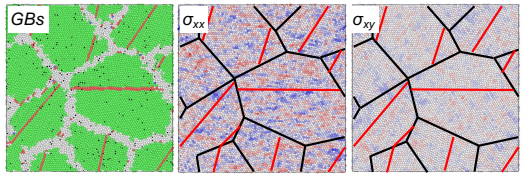

Composition Spread Islands & Micromechanics

Composition control in magnetron co-sputtering

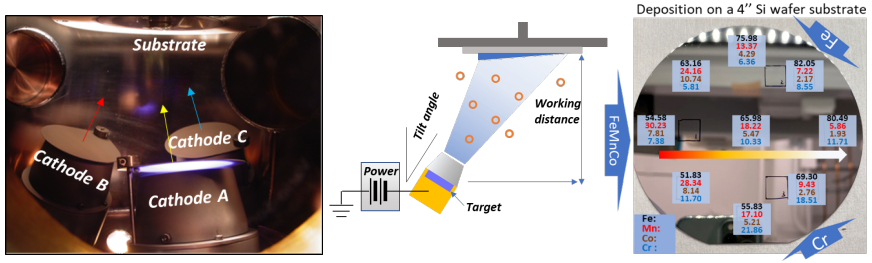

Fabrication of individual film islands

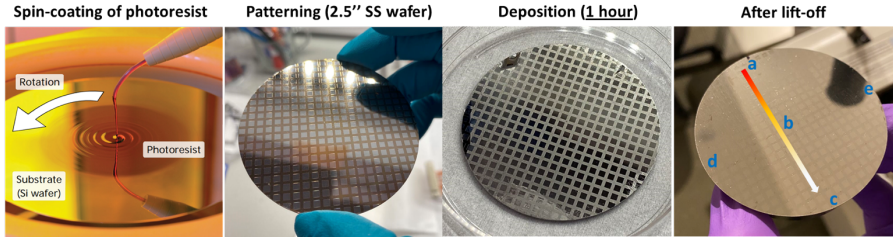

Property mapping in pristine state (H-free)

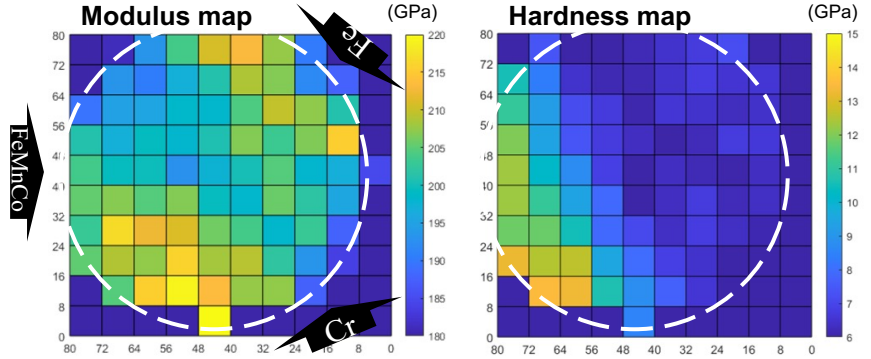

Technical Accomplishments and Progress

- Our research progress in the second year of the project was focused on both technical development of experimental and computational methodologies as well as production and high-throughput testing of the identified alloys.
- During this year we also went through the Go/No-Go decision point.
- Summary of accomplishments (detailed in following slides):

1) CALPHAD-based bulk alloy rapid screening for stacking fault energy estimation of investigated alloys
2) Development of magnetic interatomic potential for multi-element alloys
3) Investigation of Hydrogen segregation at grain boundaries via Grand Canonical Monte Carlo simulations
4) Modeling hydrogen effects on stacking fault energy with NNIP (Spin-Aware Neural Network Interatomic Potential)
5) Fabrication, compositional control and post heat-treatment of composition spread islands with micrometer thickness
6) Indentation-based high-throughput method for fracture toughness evaluation
7) Multiple Property maps for both composition and microstructure of compositional spread islands
8) Development of hydrogen mapping capabilities with required (<500 nm) spatial resolution
9) Investigation of the effect of hydrogen on the integrity of native oxide interface

Milestones accomplished

Milestone Schedule							
Milestone #	**Project Milestones**	**Type**	**Task Completion Date (Project Quarter)**				**Progress Notes**
			Original Planned	**Revised Planned**	**Actual**	**Percent Complete**	
3.1	Alloy microstructure characterization	Milestone	M15		M15	100%	The microstructural images and composition maps of the CCA composition spread were provided.
Go/No-Go #1	I. Demonstration of high-throughput characterization techniques: (i) Alloy composition spread islands (ii) H-mapping capability in SEM (iii) Reliable fracture toughness test technique in microscale II. Presentation of multiple property maps in the C-space of metastable CCAs: (i) Microstructure maps (ii) Hardness and elastic modulus maps	Go/No-Go Decision Point #1	M18		M18	100%	I. We have developed and optimized high-throughput characterization techniques: i. CSI with diameters between 50-5000 μm ii. H-mapping in SEM with resolution 10-100nm iii. Possibility of measuring fracture toughness via micropillar slitting, microcantilever bending and now also thin film bulging II. We have provided all microstructural and property maps (hardness and elastic modulus), both without and with hydrogen
5.1	H permeability characterization	Milestone	M21	M27		40%	We have caried out tests in the SEM and we will further investigate ex-situ capabilities when sample production issues are solved.
5.2	Atomistic simulation study of HE-resistance in metastable CCAs	Milestone	M24	M27		100%	We have developed a SANNIP for the Co-Cr-Fe-Mn-H system and obtained promising preliminary results. We have also started MC simulations of oxide layers.
4.2	Fracture toughness measurement in microscale	Milestone	M27			20%	We have identified bulge test and indentation-based methods as promising techniques.
6.1	Microstructure characterization of produced alloys	Milestone	M30			40%	We have begun simulation-guided bulk production of alloys that are already used in commercial applications (specifically, martensitic stainless steel)

Technical Accomplishments and Progress:

CALPHAD-based high-throughput alloy screening

Calculation	TC	Model	Empirical
Alloy system	TCFE11	Fe, Cr, Ni, Al, Mn, Mo, C, Co, Si	Fe, Cr, Ni, Mn, Mo, Si, C, N
Average difference (J/m²)	0.23	0.017	0.013
Standard Error (J/m²)	0.01	0.0014	0.0028

SFE* calculation methods

- $\gamma_{SFE} = 2\rho\,\Delta G^{\gamma\rightarrow\varepsilon} + 2\sigma$ (Olson-Cohen [1])

  σ: γ/ε interfacial energy (treat as constant)
  ρ: {111} plane number density (constant)

  Gibbs free energy obtained with:

  - ThermoCalc – TCFE11
  - Gibbs energy modeling for $\Delta G^{\gamma\rightarrow\varepsilon}$ [2]

- Empirical SFE formula [3]

(for details of the model equations please refer to the Technical Backup slides)

SFE* calculation methods validation

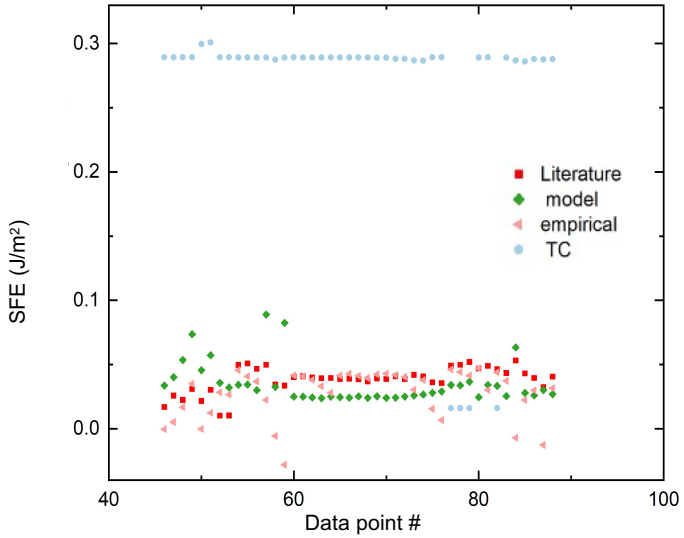

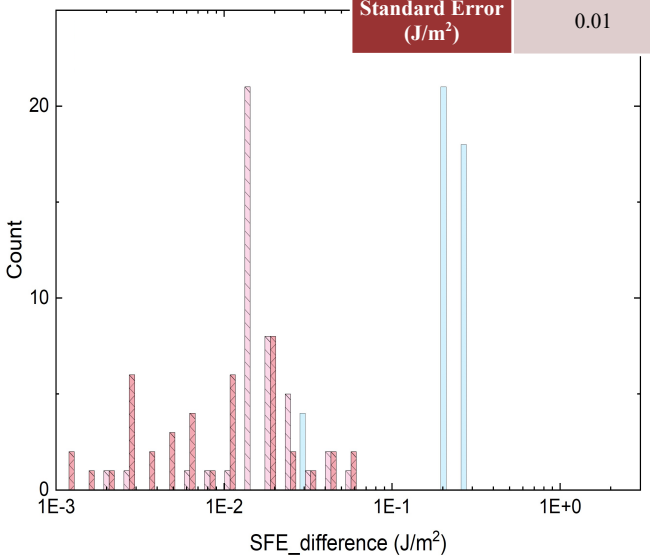

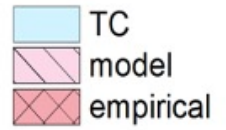

SFE: Stacking Fault Energy

Alloy SFE model to current thin film m-HEA system

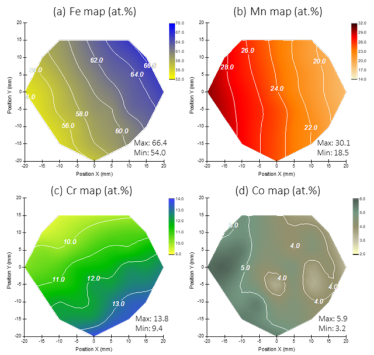

	Temperature/ °C	Fe	Cr	Mn	Co
Min	750	Bal	9	14	2
Max	750	Bal	14	32	6

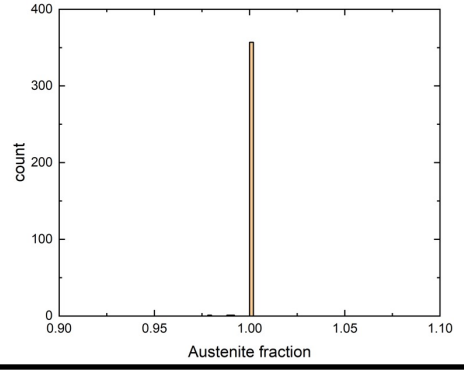

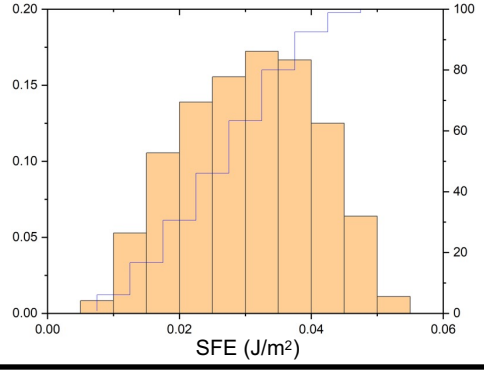

- Developed model to predict SFE of austenite
- Current Gibbs energy model matches the accuracy as the empirical formula
- Current Gibbs energy model includes all elements of interest: Fe, Cr, Ni, Cr, Co, Mn, etc.

[1] Olson, Gregory Bruce, and Morris Cohen. "A general mechanism of martensitic nucleation: Part I. General concepts and the FCC→ HCP transformation." Metallurgical Transactions A 7.12 (1976): 1897-1904.
[2] Xiong, Wei, et al. "An improved magnetic model for thermodynamic modeling." Calphad 39 (2012): 11-20.
[3] Dai, Q. X., et al. "Structural parameters of the martensite transformation for austenitic steels." Materials characterization 49.4 (2002): 367-371

Taşan Group

CALPHAD-based high-throughput alloy screening

Target material & processing

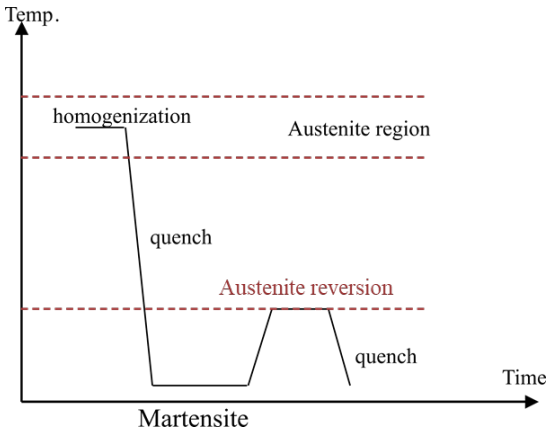

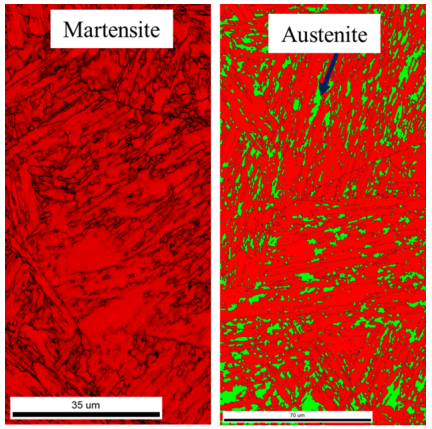

Austenite reversion

Composition screening framework

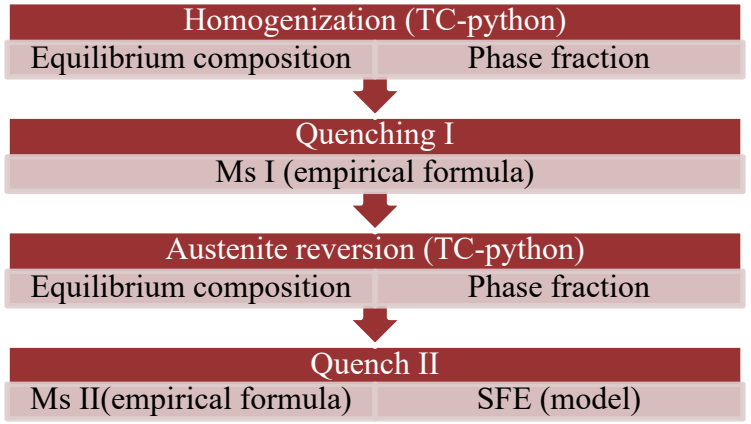

Screening :
- Starting composition
- Austenite reversion temperature

Boundary condition
- Ms I > 200 °C
- Ms II < 50 °C
- Austenite fraction 0.2-0.5

Composition screening

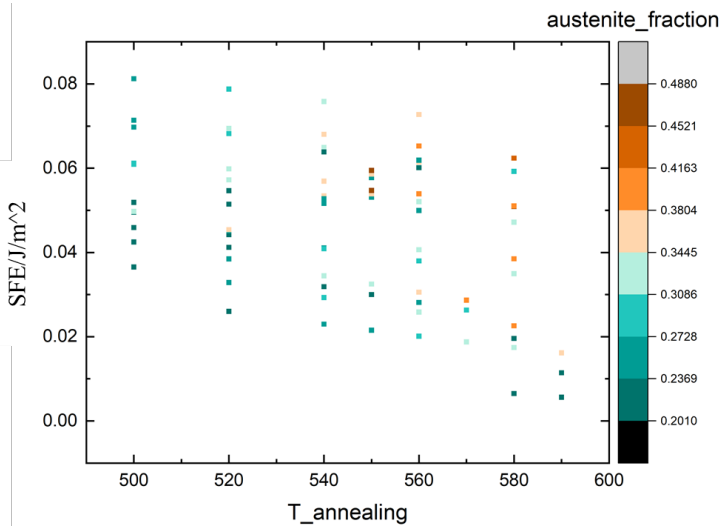

	Min	Max
Temperature/ °C	400	800
Fe	Bal	Bal
Cr	10	20
Ni	0	15
Mn	0	15
C	0	0.1
Al	0	5
Co	0	15

Composition refinement and alloy design

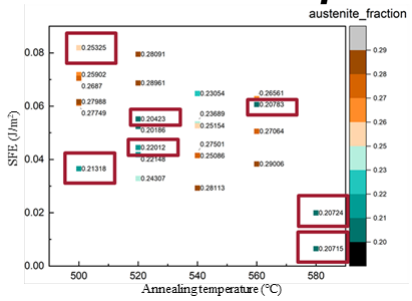

Extra filter:
$\gamma \in [0.2,0.3]$
Elements: Fe-Cr-Ni-Al-Co-Mn

Target: varying SFE with similar γ

Composition						SFE	γ%	Annealing
Fe	Cr	Ni	Mn	Co	Al	(mJ/m²)		(°C)
59	13	12	0	15	1	81	25	500
67	13	9	0	10	1	60	20	560
67	13	6	3	10	1	55	20	520
71	13	6	3	6	1	44	22	520
77	13	6	3	0	1	37	21	500
77	13	6	3	0	1	20	21	580
80	13	0	6	0	1	7	21	580

- Developed framework to screen wide composition range
- Achieved composition selection based on desired properties

Magnetic Interatomic Potential for Multi-Element Alloy

- Framework: interatomic potential including magnetic degree of freedom

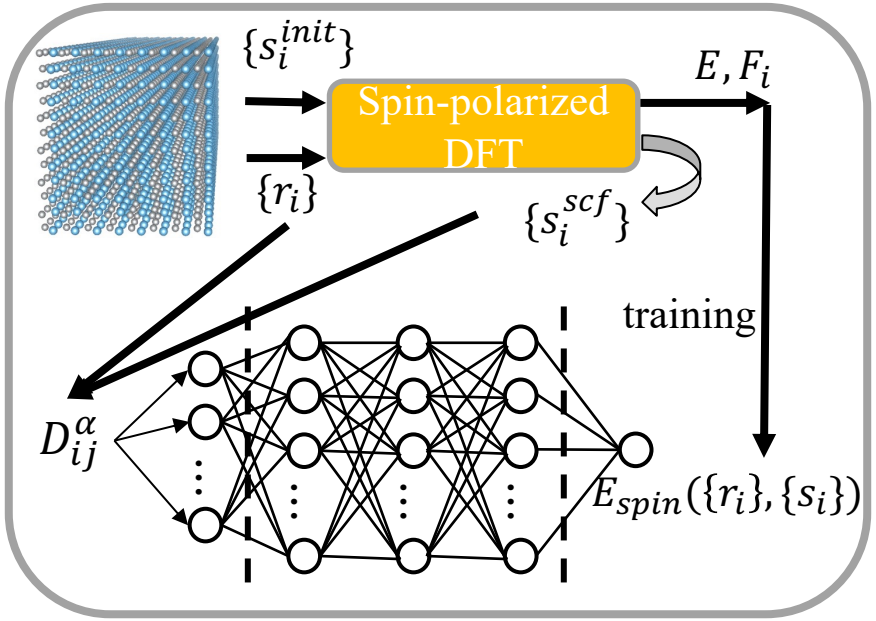

Validation through pure iron

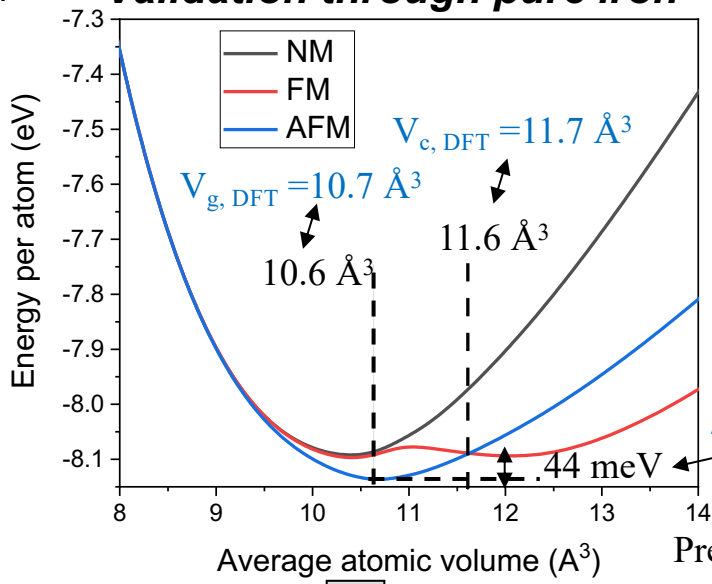

Example: $\gamma - phase$, well consistent with DFT

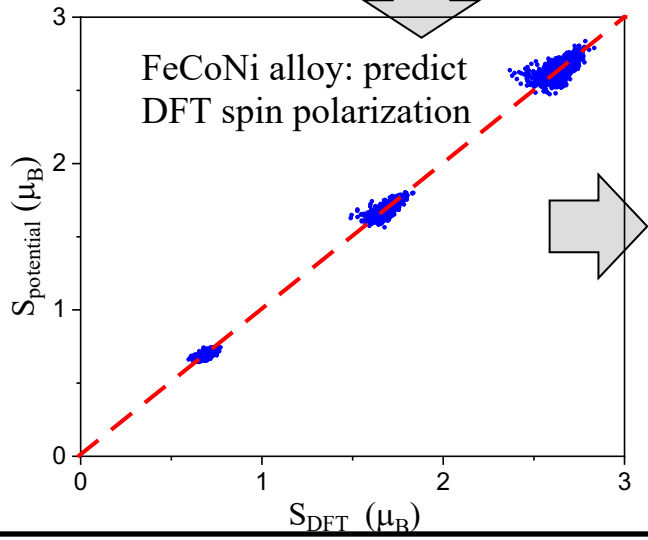

Predict composition-dependent saturate magnetism of $Fe_{1-x-y}\,Co_xNi_y$ M_s

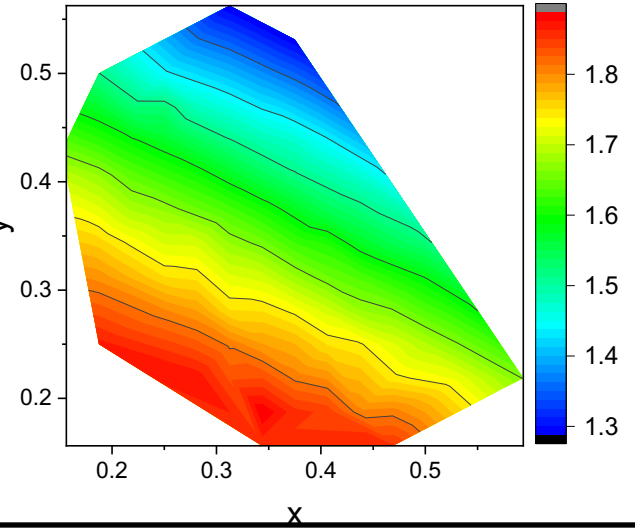

- Constructed spin-aware potential:
  - Avoid spin-noise in potential training
  - Predicting magnetic properties M_s, H_c, T_c during MD simulation
- Apply to materials systems:
  - Validation: reproduce DFT magnetic phase curve for Fe
  - Application: FeCoNi multi-element magnetic alloy

Chemically Defeating H Segregation at Grain Boundaries

Snapshots represent the equilibrium H atoms distributions
as obtained from hybrid MD-GCMC (Grand Canonical Monte Carlo) Simulations under the same H chemical potential

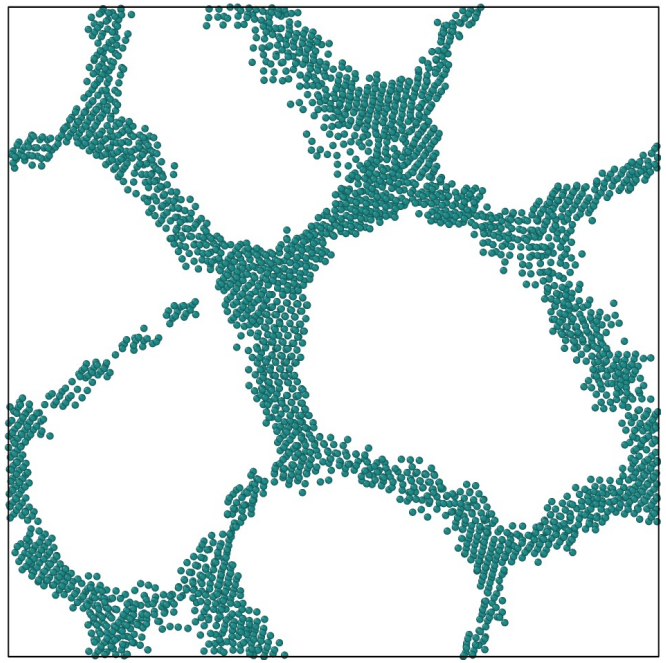

Pure Ni: H segregation at GBs

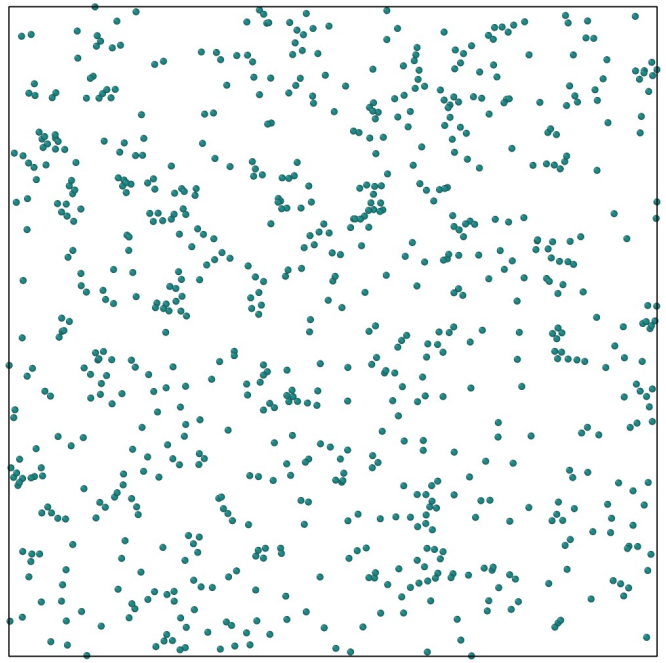

NiAl random solution: uniform distribution of H

- H segregation at GBs in elemental metals or dilute alloys often lead to embrittlement
- It is challenging to prevent such GBs segregation of H
- However, in an equimolar NiAl random solid solution, H atoms can uniformly distribute
- Suggest possible ways to prevent GBs segregation of H by designing complex concentrated alloys

*Modeling H Effects on Stacking Fault Energy (SFE) with NNIP**

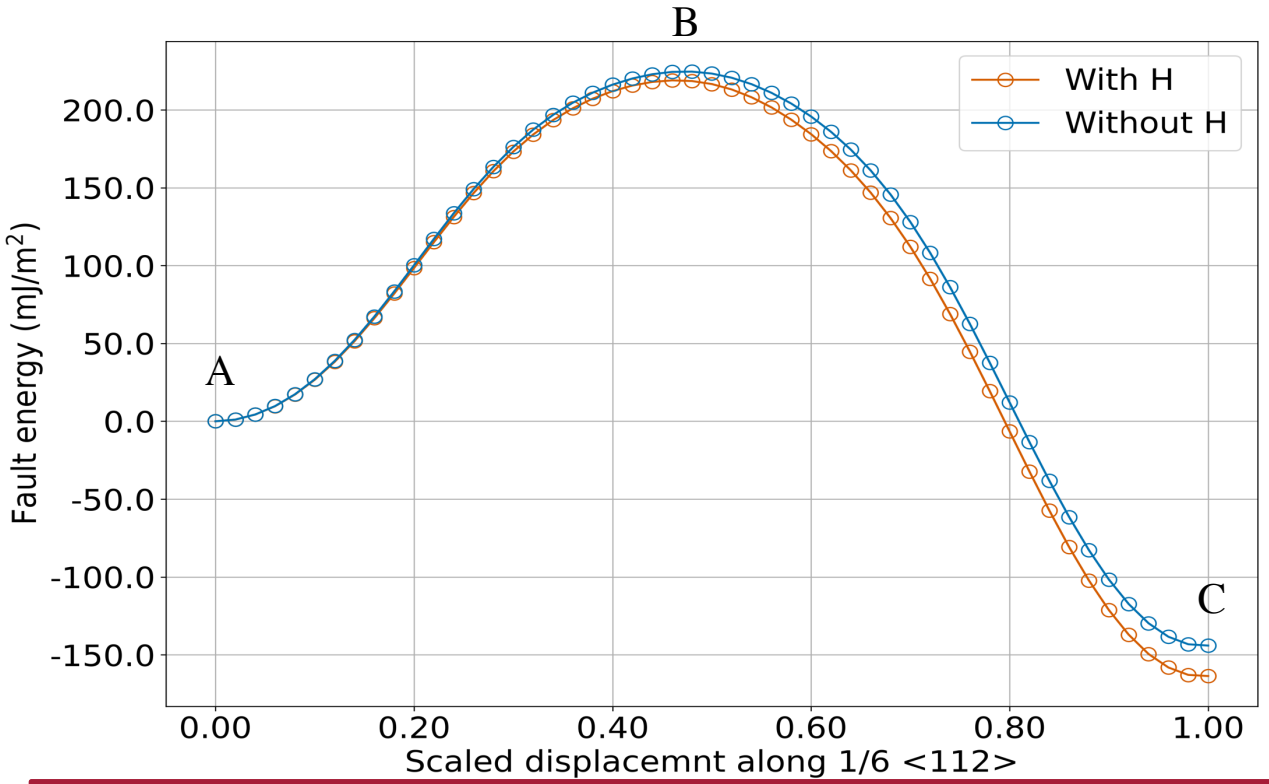

- Our experiments demonstrated dramatic effects of H on microstructure changes
- H charging leads to stacking fault and HCP phase formation
- Our NNIP-based calculations suggest a reduction of intrinsic SFE (~20 mJ/m^2) with addition of H
- Decreased SFE due to H can be a driving force for experimentally observed microstructure change

NNIP-based generalized stacking fault energy (GSFE) calculation on a HEA system $Co_{0.1}Cr_{0.1}Fe_{0.45}Mn_{0.35}$

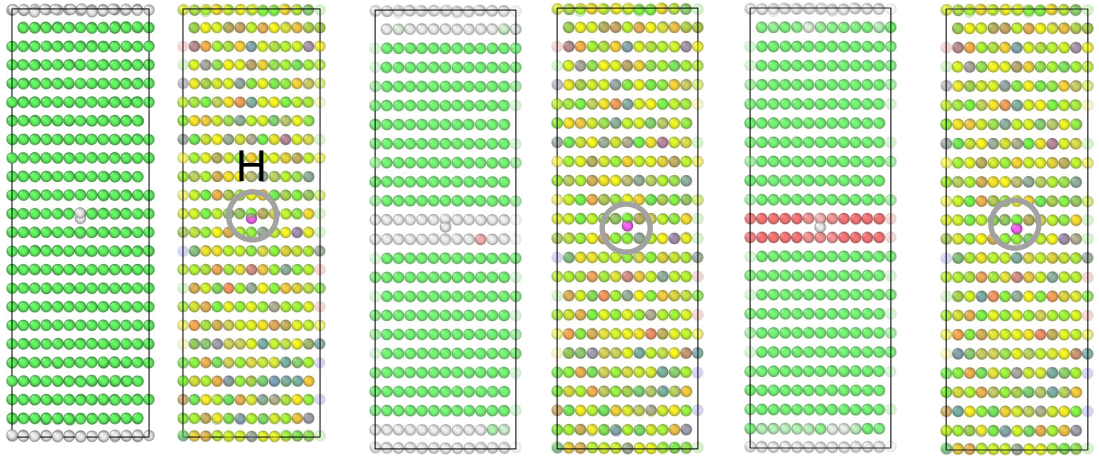

A: Initial state B: Unstable SF C: Intrinsic SF

- A single H atom is inserted on the slip plane
- GSFE curve was obtained by rigid shear along <112> direction, allowing relaxation in slip plane normal direction
- Snapshots represent the initial perfect FCC structure (A), unstable stacking fault (B), and intrinsic stacking fault(C)
- For each pair of snapshot:
  - Left: defect analysis (white-defective atoms, red-stacking fault atoms, green-FCC atoms)
  - Right: element distributions (H is marked with circle)

*NNIP: Neural Network Interatomic Potential

Micrometer-thick compositional spread islands (CSI)

Fabrication of micromwrwe-thick CSI

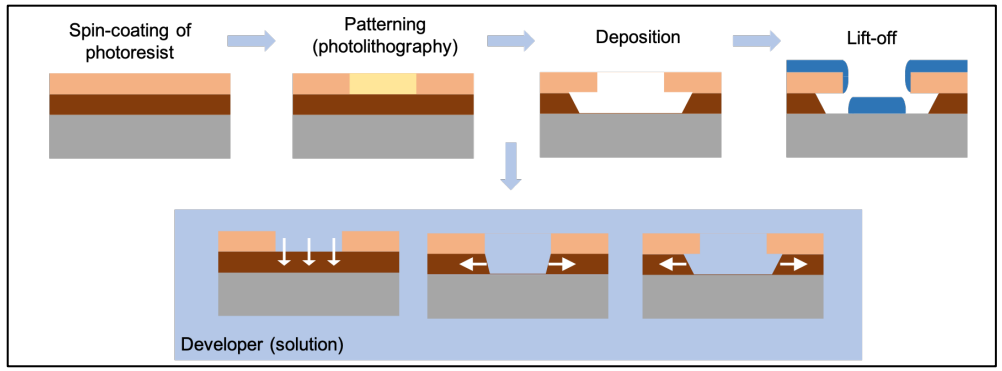

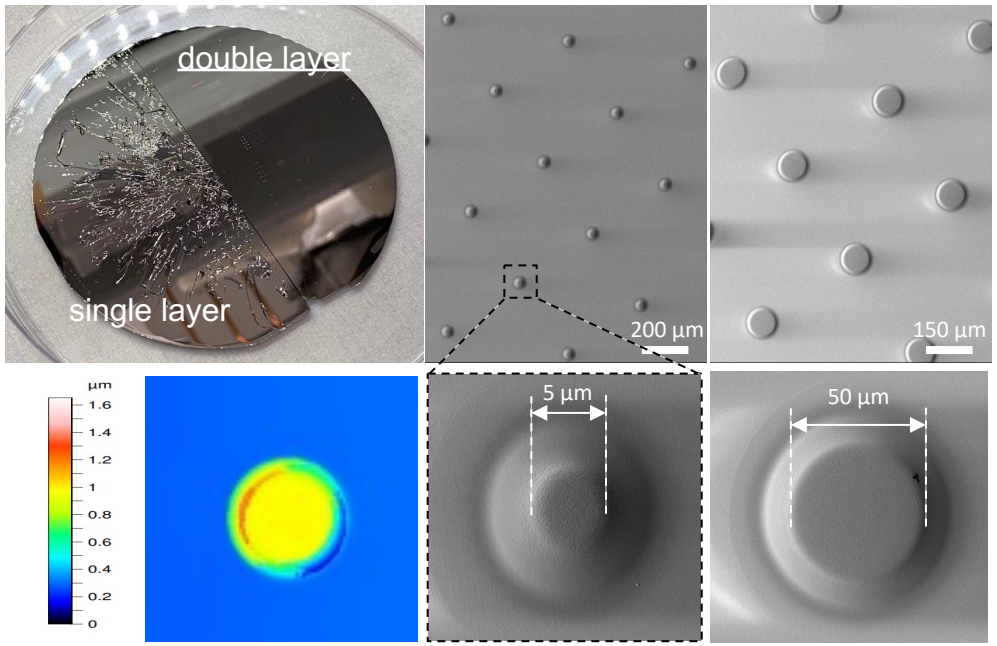

- Micron-thick CSI with tunable size and shape without delamination

In situ H-charging setup for nanoindentation

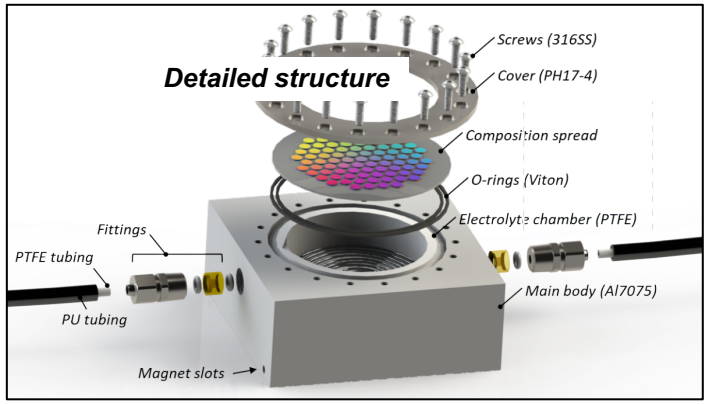

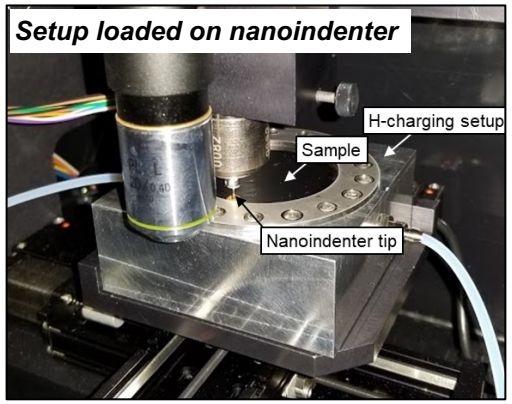

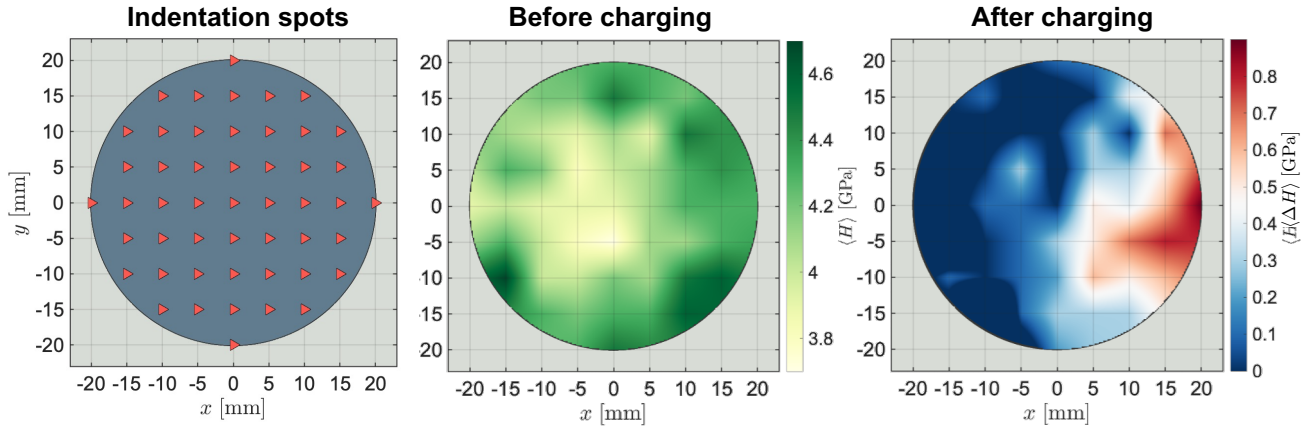

- Developed an analytical method to exclude the space-varying compliance introduced by substrate deflection
- Hardness variation due to H-charging is evaluated across a large composition space in a high-throughput manner
- Fe-rich region shows more pronounced hardness improvement after charging

Indentation-based HT method for fracture evaluation

Indentation on brittle substrate

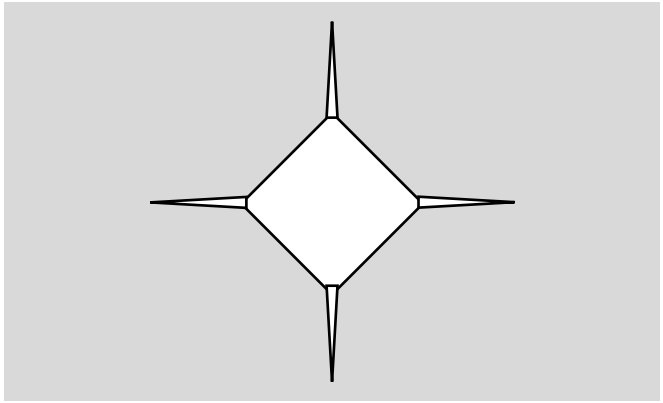

Quartz (Z-cut)

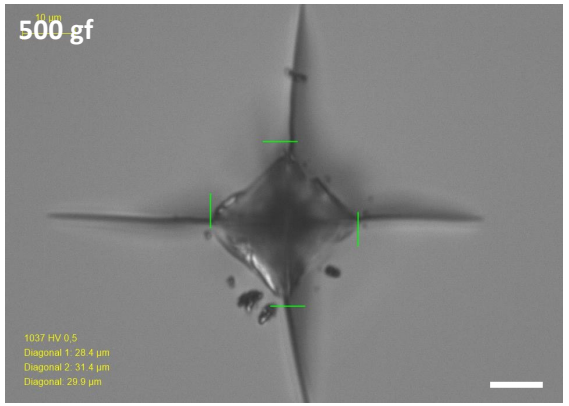

Fused silica

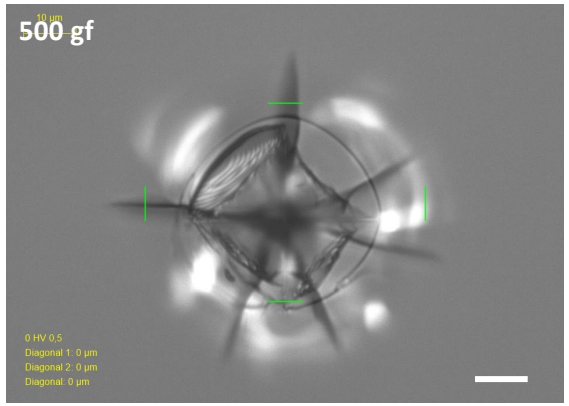

Si

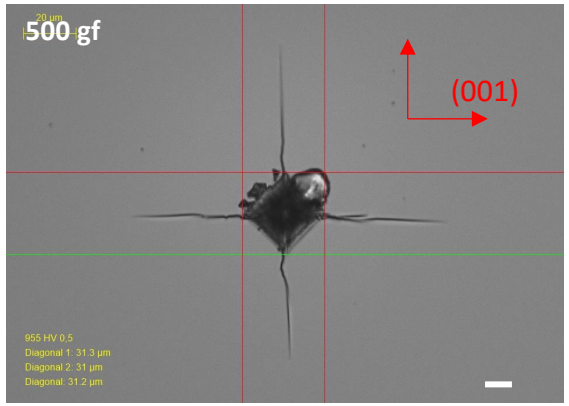

10 µm

Indentation on *brittle* film on brittle substrate

Si substrate

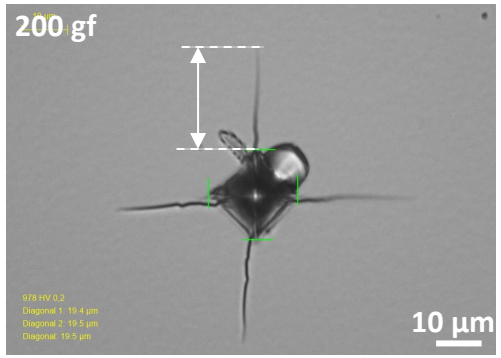

Brittle (as-deposited) HEA film on Si

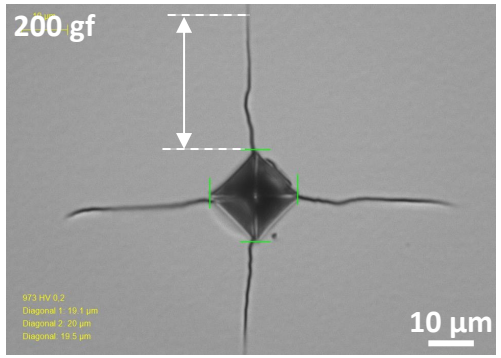

Indentation on *ductile* film on brittle substrate

Ductile (annealed) HEA film on z-cut quartz

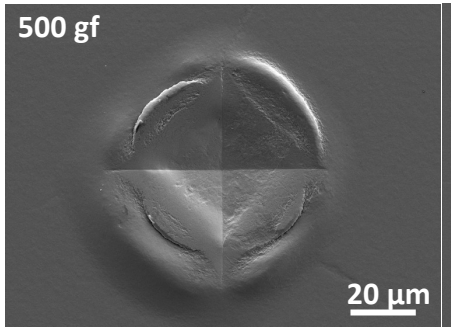

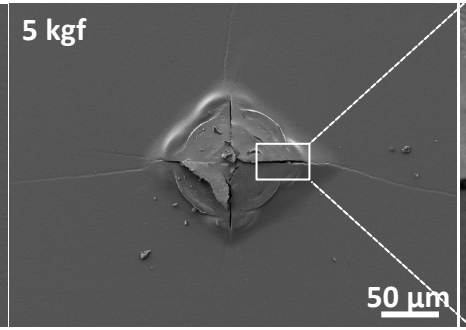

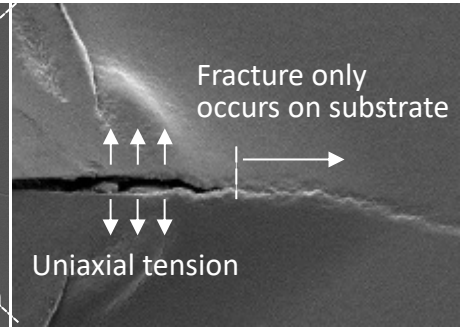

- The brittleness/toughness can be assessed through the crack length
- Multiple types of substrate are investigated, quartz substrate is selected for its brittleness and CTE similarity with the alloy film
- For brittle film, the toughness can be analyzed to quantitate level
- For ductile film, crack front is strained uniaxially, which can be used to evaluate ductility and deformation mechanism

Multiple Property maps: Composition and Microstructure

*Thin film **with** diffusion barrier*

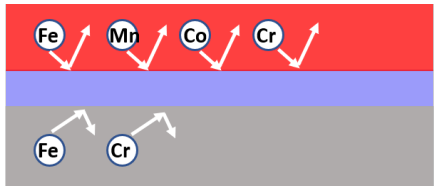

FeMnCoCr film

HfO_2 (30nm)

430 SS substrate

Compositional Maps via EDS

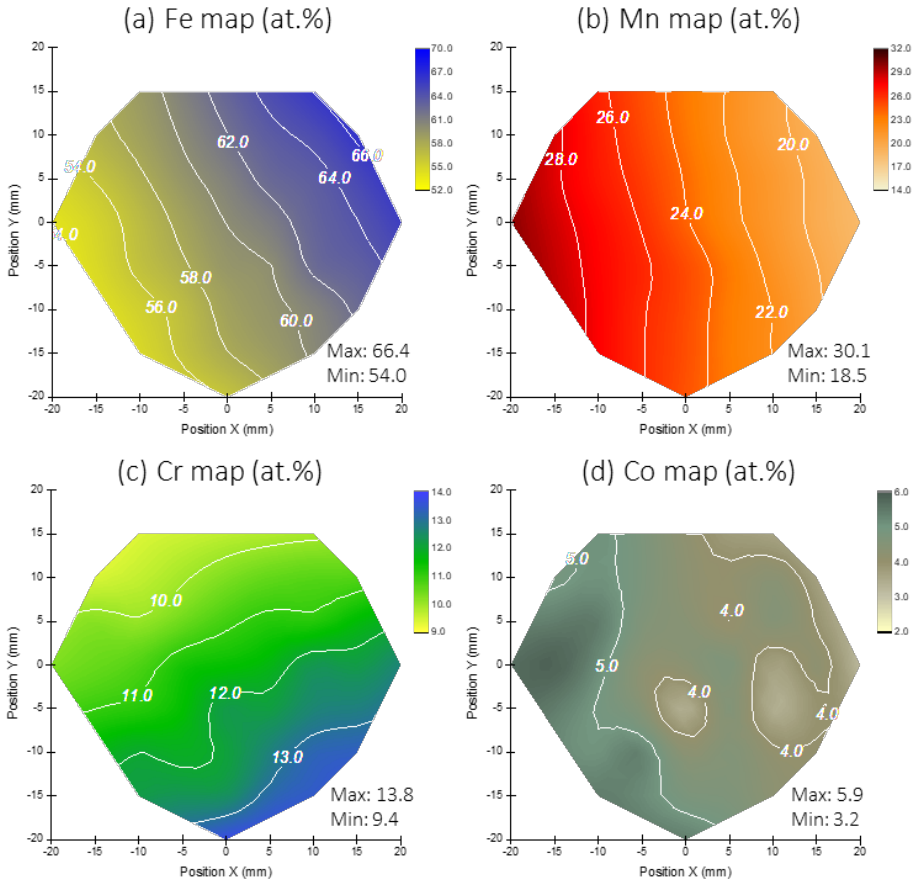

EBSD Maps: IPF and grain size

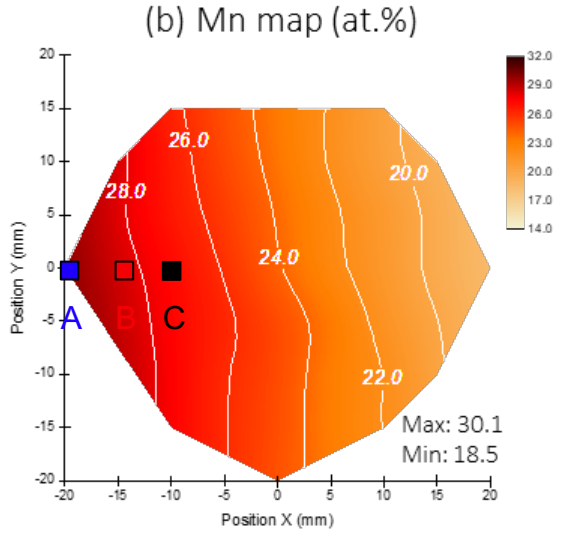

Grain size distribution

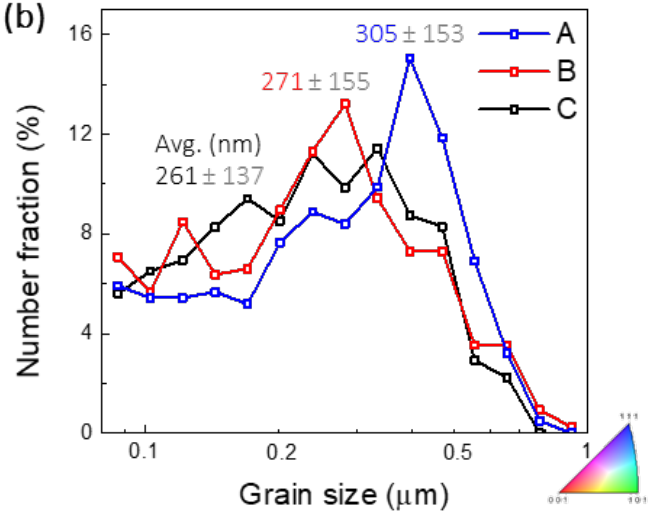

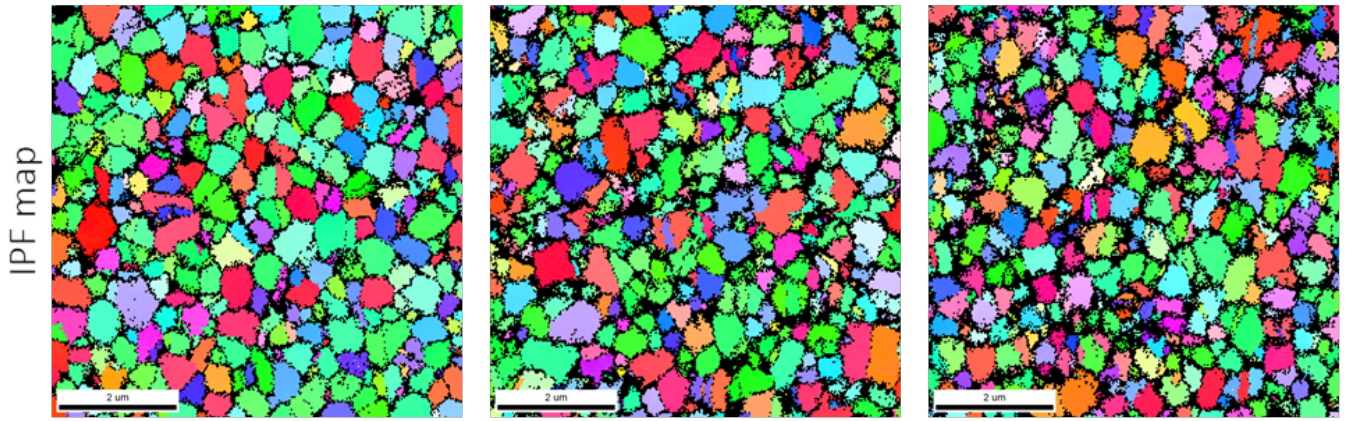

(c) Composition A: $Fe_{53.9}Mn_{30.1}Cr_{10.3}Co_{5.7}$

(d) Composition B: $Fe_{55.1}Mn_{28.5}Cr_{10.5}Co_{5.9}$

(e) Composition C: $Fe_{56.8}Mn_{27.3}Cr_{10.7}Co_{5.2}$

- Complete characterization of CSI thin films

Taşan Group

Hydrogen Mapping with High Spatial Resolution

1) Improved silver reduction and decoration technique: New Method

Model stainless steel with well-defined cellular structures

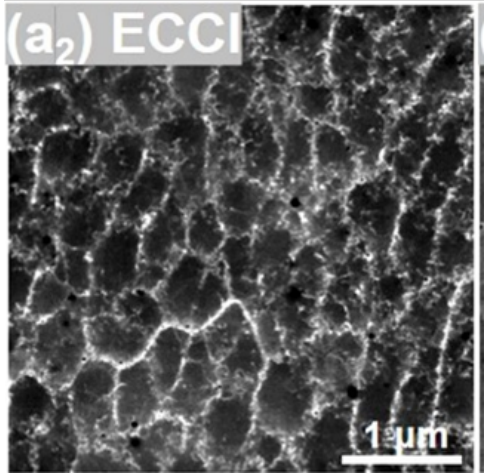

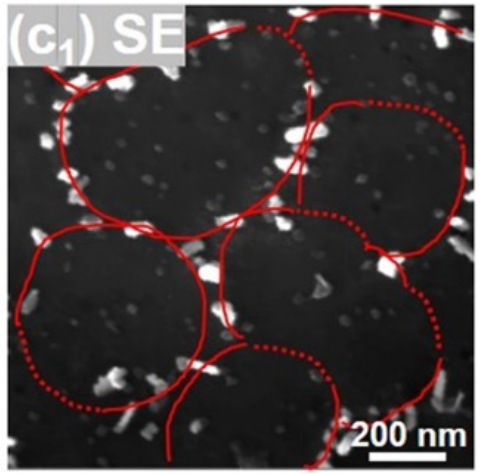

By tuning:
- Concentration of $K[Ag(CN)_2]$
- Immersion time
- Light exposure

Issues Resolved:
- Ag particles < 100 nm)
- Inaccuracy ("false positive")

- Nm size silver particles
- Negligible silver deposition without hydrogen

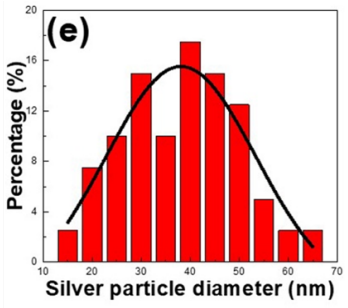

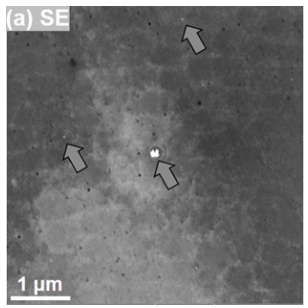

2) Hydride-forming nanoparticles mapping technique: New Method

- Certain transition metals form hydrides upon exposure to hydrogen
- Palladium is particularly known to be "H sponge"
- Upon hydride formation → large change in volume

Our Hypothesis: Pd Nanoparticles (NPs) distributed on sample surface will change size as sample is H-charged

Electro-deposition:
- 5g/L PdCl2 in distilled water + NH4OH 30%
- 20min deposition at -1V

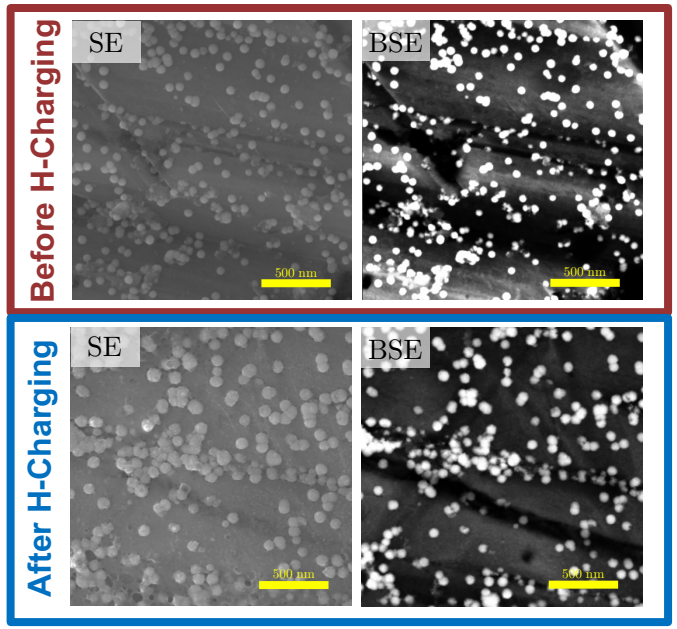

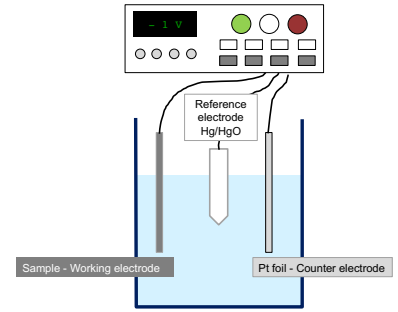

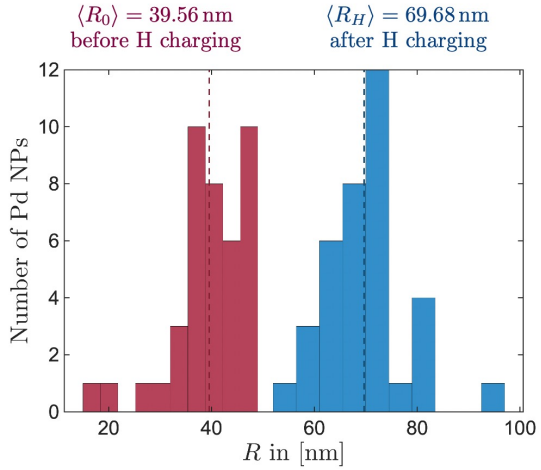

- Developed multiple hydrogen mapping techniques with required resolution

Effect of hydrogen on integrity of Al_2O_3/Al interface

Equilibrium structure and propagation of the Al_2O_3/Al interface during Al_2O_3 growth on Al was identified using ab initio GCMC.

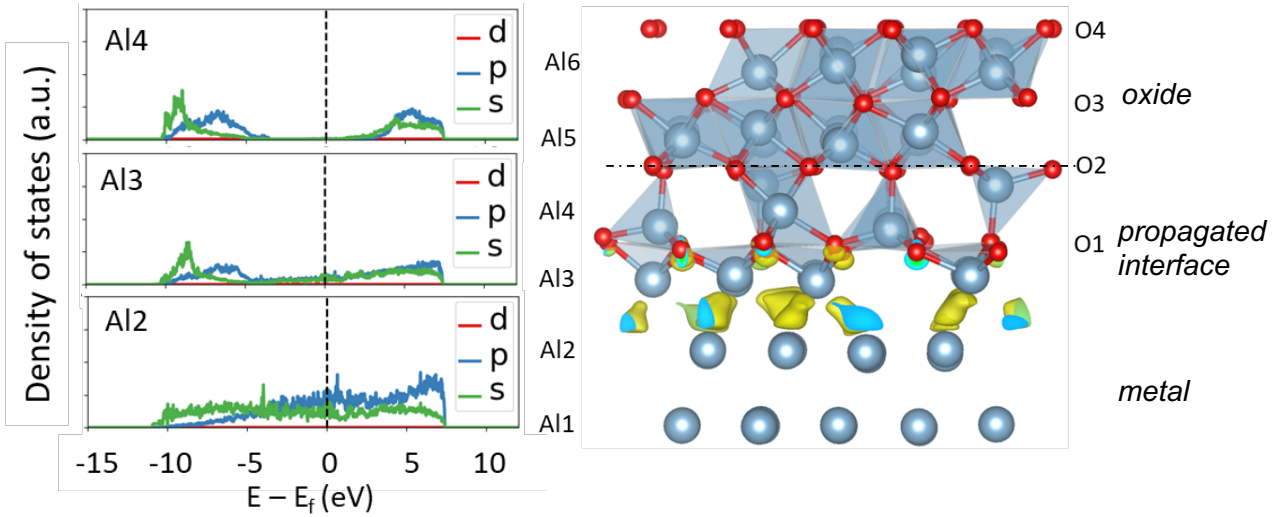

- Incorporation of 1 layer of O (O1) at the interface nearly introduces a bandgap in layers Al3 and Al4 of Al metal. Under-coordinated Al atoms introduce a high density of Al 3sp mid-gap states in layer Al3.
- The Al 3sp mid-gap states dictate oxygen incorporation in the next layer of Al, causing **layer-by-layer propagation** of the oxide into the metal.
- The rapid reduction in density of states at the Fermi level prevents charge transfer necessary for further corrosion, resulting in the **self-healing property** of this common corrosion barrier system.
- This understanding can be **extended** to understanding and engineering the growth of other passivating oxides on metals.

Effect of various hydrogen and aluminum vacancy defects on interfacial barrier performance and integrity was studied

Excess charge at interface due to under-coordinated Al

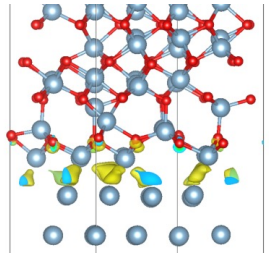

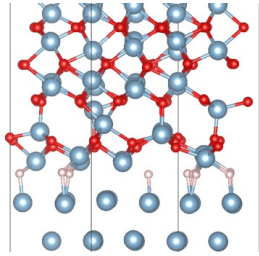

Hydrogen occupies sites with this excess charge ('H_O' defect)

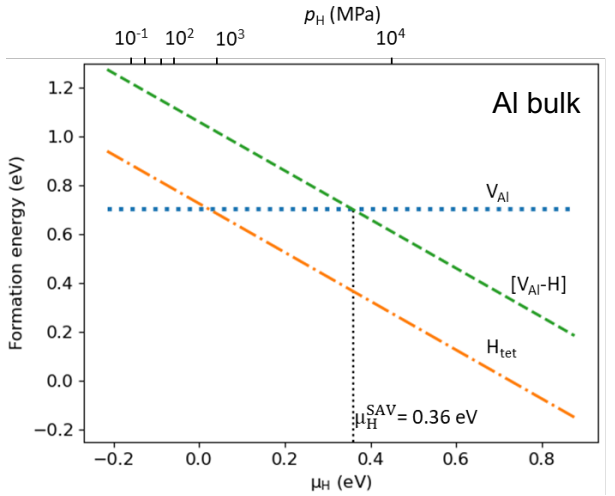

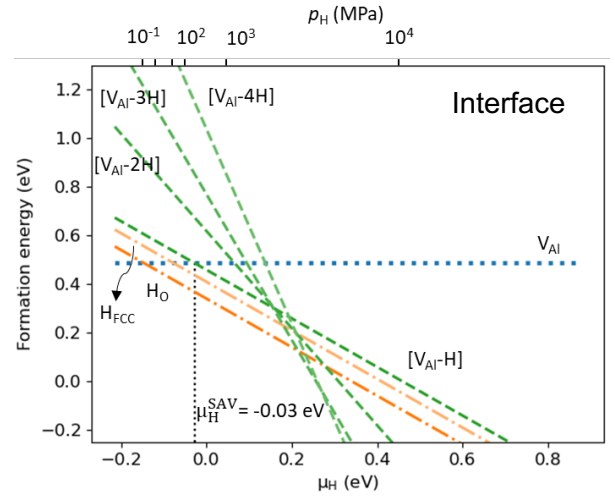

- Presence of Al dangling bonds at interface leads to **hydrogen trapping at the interface** due to the formation of strong Al-H bonds ('H_O' defect) -> Al_2O_3/Al multilayer coatings could be effective hydrogen barrier coatings, while providing superior mechanical properties
- However, hydrogen at the interface reduces chemical potential of superabundant vacancy (SAV) onset -> this could lead to **cavity formation and embrittlement** of the interface

Collaboration and coordination

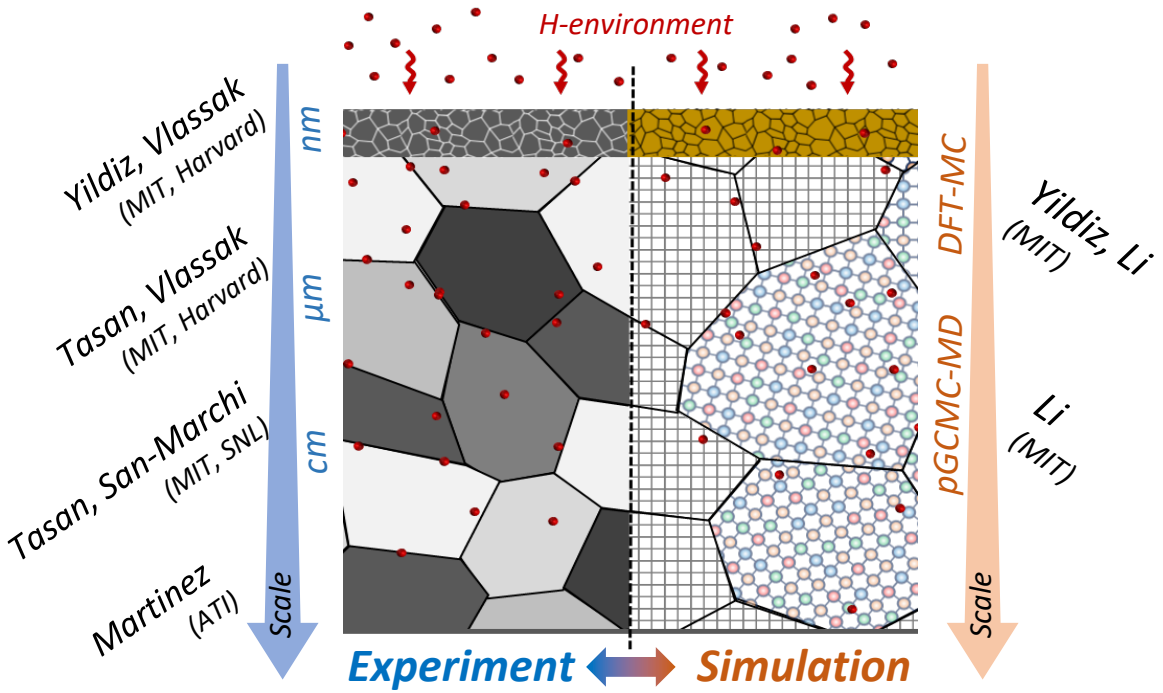

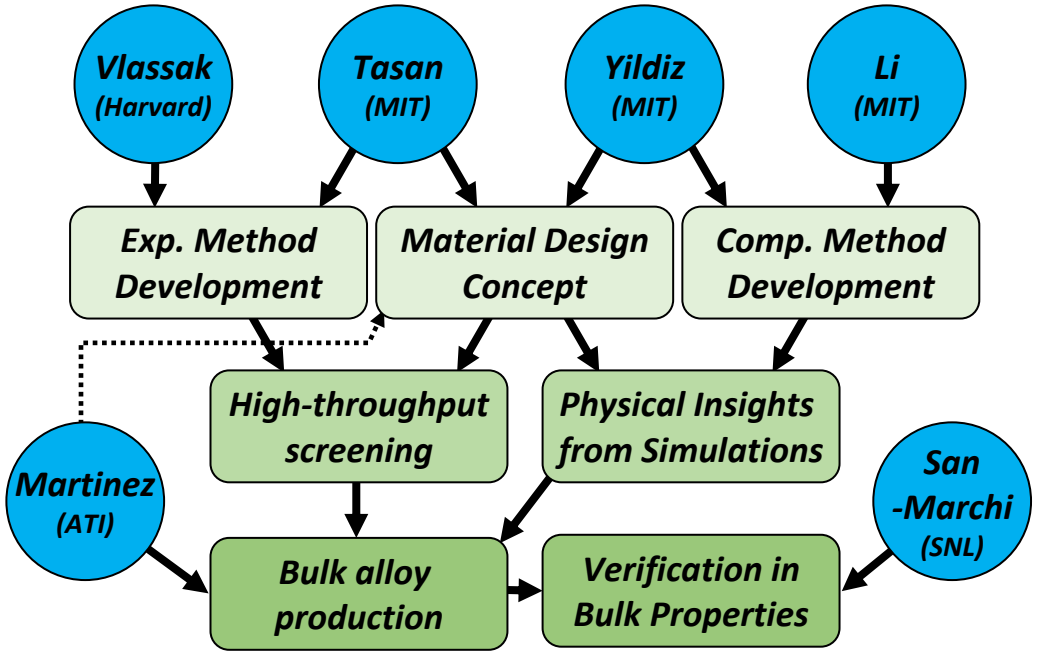

Team members and partners	Project roles
Tasan Group, MIT	Project lead, Management/coordination, Setup design, Alloy design, Experimental methodology development, Bulk alloy production
Li Group, MIT	Computational technique development, Interatomic potentials development
Yildiz Group, MIT	Surface structure and property characterization, Computational technique development,
Vlassak Group, Harvard University	Composition spread film fabrication, Heat treatment, Micromechanical testing, Experimental methodology development
ATI (Unfunded industrial partner)	Bulk alloy production, Consultant on alloy system selection, production and industrial requirements
Sandia National Lab. (H-Mat partner)	Bulk alloy testing in high-pressure hydrogen environment (planned for Year 3)

Remaining Challenges and Barriers

Category	Remaining challenges and barriers	Planned resolution
Composition spread island fabrication	Minimize the number and size of the ~100 nm oxides particles distributed on the top surface of samples after annealing.	Optimize heat treatment conditions and barrier coatings.
Micromechanics-based high-throughput screening with in situ H-charging	Fracture toughness measurement with microscale alloy specimens.	Binary testing using indentation cracking or bulge tests, and verify with bulk alloy.
	Bridging micromechanical test results and bulk alloy characteristics.	Complement effects of defects and boundaries based on computational approach and bulk testing.
Computational framework for multi-component alloys	Large dataset size required for a potential as complex as FeMnCoCr-H.	Start with a small island in composition space and sample the geometric and spin configuration subspaces.
	The magnetic NNIP is restricted to pre-set magnetic phases (e.g., a ferromagnetic phase) to which the spin polarized DFT stably converge.	Test NNIP trained by the DFT with random magnetization.

Proposed Future work

- Proceed with bulk production of the CALPHAD-designed alloys with different SFE.
- Develop and implement a high throughput characterization of the bulk samples through micro-indentation as a way to identify the underlying microstructure without the need of time-consuming SEM imaging. We will combine this with uniaxial mechanical testing before and after H-charging.
- Apply nanoindentation-based methods for high-throughput toughness and deformation mechanism evolution/screening at the micro- and nano-scale together with H-permeability.
- Extend the NNIP trained by DFT calculation to all magnetizations; Apply the potential to study magnetic properties of multi-element alloy controlled by compositions, temperature, and pressure through MD simulations.
- Combine active learning, hybrid MD-GCMC (Grand Canonical Monte Carlo) simulations, and first-principles calculations to systematically generate a large data set that can be used to address defects-H interactions with and without chemical short-range ordering.
- Bulk alloy testing in high-pressure hydrogen environment at SANDIA National Lab (H-Mat partner).

Summary

- A CALPHAD-based bulk alloy screening approach was utilized to determine the stacking fault energy of the investigated alloys and guide bulk production.
- Fabrication techniques for composition spread islands with micron-thickness have been developed, and a full characterization of the local composition (via EDS), microstructure and grain size (via EBSD) has been provided.
- Two different methodologies for hydrogen mapping with nanometer scale (< 500nm) resolution were developed and implemented on different alloys.
- A spin-aware neural-network-based interatomic potentials for complex concentrated alloys was established and used to understand the role of hydrogen at grain boundaries as well as the role of hydrogen on stacking fault energy. A magnetic interatomic potential for multi-element alloys has also been developed and tested.
- A simulation framework to study native oxides has been established and tested with respect to the Al2O3/Al interface as a base for future studies on an Fe-Cr like the HEA used in this study.

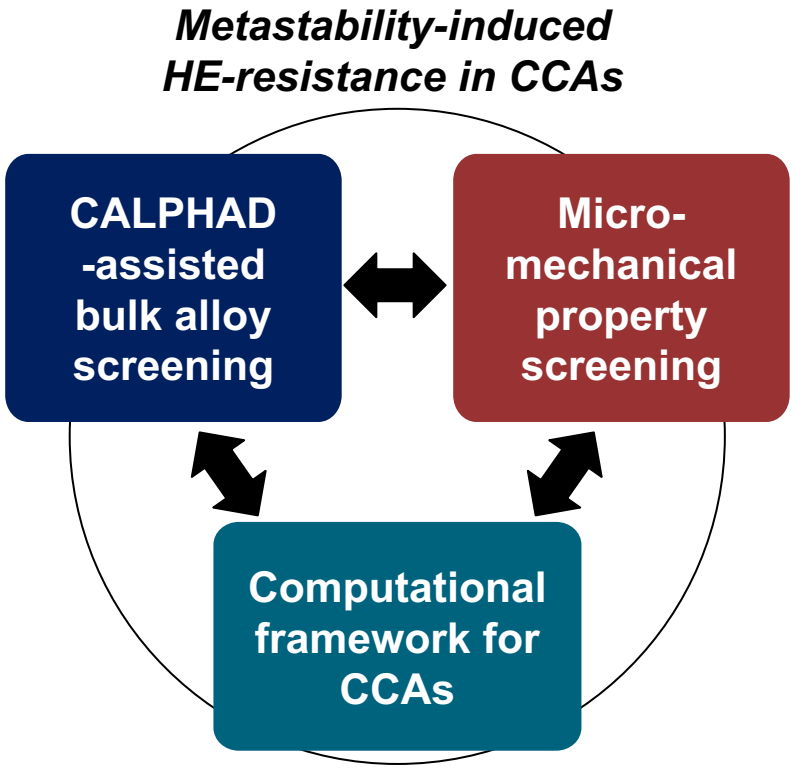

Technical Backup and Additional Information

Technology Transfer Activities

- No patent application is filed in this project yet. Once the high-throughput alloy design technology is matured and novel alloy compositions with high HE-resistance are discovered, patent applications for the results will be filed.
- The project team is continuously interacting with the unfunded industrial partner, ATI. Alloy manufacturing and application experts from ATI has been joining the regular progress update meetings of the project team (quarterly) and sharing opinions on alloy system selection and industrial requirements.

Progress toward DOE Targets or Milestones

- This project is focused on developing a novel high-throughput alloy design strategy for the discovery of alloys with superior HE-resistance. The final goal of the project is the verification of the high-throughput alloy design strategy, including the confirmation of high HE-resistance of discovered alloys by comparing yield strength and fracture toughness between specimens in 100 MPa-H_2 condition vs. in air.

- This project will contribute to the following DOE technical tasks and milestones from the "3.3. Hydrogen Storage" section of the Hydrogen and Fuel Cell Technologies Office Multi-Year Research, Development, and Demonstration Plan.

Task 1. Material Discovery

- Perform theoretical modeling to provide guidance for materials development.

- Determine the H2 storage capacity of potential storage materials and demonstrate reproducibility of their synthesis and capacity measurements

Milestone 1.1. Material Handling: Determine applicability of H_2 storage materials for material handling applications.

Milestone 1.3. Material Handling: Down-select H_2 storage materials for material handling applications.

Technical Backup:
SFE Calculation methods: details

SFE calculation methods

- $\gamma_{SFE} = 2\rho\,\Delta G^{\gamma\to\varepsilon} + 2\sigma$ (Olson-Cohen [1])

  σ: γ/ε interfacial energy (treat as constant)
  ρ: {111} plane number density (constant)

  – ThermoCalc – TCFE11

  – Gibbs energy modeling for $dG^{\gamma\to\varepsilon}$

- Empirical SFE formula [2]

$$\gamma^{300}\ (\mathrm{mJ/m^2}) = \gamma^0 + 1.59\mathrm{Ni} - 1.34\mathrm{Mn} + 0.06\mathrm{Mn}^2 - 1.75\mathrm{Cr} + 0.01\mathrm{Cr}^2 + 15.12\ \mathrm{Mo} - 5.59\mathrm{Si} - 60.69\ (\mathrm{C} + 1.2\mathrm{N})^{0.5} + 26.27\ (\mathrm{C} + 1.2\mathrm{N})(\mathrm{Cr} + \mathrm{Mn} + \mathrm{Mo})^{0.5} + 0.61\ [\mathrm{Ni}(\mathrm{Cr} + \mathrm{Mn})]^{0.5}$$

(where γ^{300} is the value of *SFE* at room temperature and γ^0 is the value of *SFE* of pure austenitic iron at room temperature.)

Gibbs energy modeling

$$\Delta G^{\gamma\to\varepsilon} = \Delta G^{\gamma\to\varepsilon}_{mag} + \Delta G^{\gamma\to\varepsilon}_{chem}$$

$$G^{\phi}_{chem} = \sum x_i G^{\phi}_i + \sum x_i x_j \Omega^{\phi}_{i,j}$$

$$G^{\phi}_{mag} = RT\ln(\beta^{\phi}+1)\,f(\tau^{\phi})$$

x_i : atomic fraction
G^{ϕ}_i: molar Gibbs energy of element *i* of phase ϕ
$\Omega^{\phi}_{i,j}$: molar excess Gibbs energy of element *i, j* of phase ϕ
β^{ϕ}: mean magnetic moment of phase ϕ
$\tau^{\phi} = \frac{T}{T^{\phi}_{Neel}}$, T^{ϕ}_{Neel}: Neel temperature of phase ϕ

$$\mathrm{f}_{Xiong}(\tau) = \begin{cases} 0, \tau < 0 \\ 1 - \frac{1}{D} * [\frac{0.38438376}{t*p} + 0.63570895 * \left(\frac{1}{p} - 1\right) * \left(\frac{t^3}{6} + \frac{t^9}{135} + \frac{t^{15}}{600} + \frac{t^{21}}{1617}\right)], 0 < \tau < 1 \\ -\frac{1}{D} * (\frac{t^{-7}}{21} + \frac{t^{-21}}{630} + \frac{t^{-35}}{2975} + \frac{t^{-49}}{8232}), \tau > 1 \end{cases} \quad [3]$$

[1] Olson, Gregory Bruce, and Morris Cohen. "A general mechanism of martensitic nucleation: Part I. General concepts and the FCC→ HCP transformation." Metallurgical Transactions A 7.12 (1976): 1897-1904.
[2] Dai, Q. X., et al. "Structural parameters of the martensite transformation for austenitic steels." Materials characterization 49.4 (2002): 367-371
[3] Xiong, Wei, et al. "An improved magnetic model for thermodynamic modeling." Calphad 39 (2012): 11-20.

Technical Backup:

SANNIP (Spin Aware Neural Network Interatomic Potential)

$$E(\{r_i, s_i\}) = E_0^{NN}(\{r_i\}) + \left[\sum_i \left(\alpha_i^1 |s_i|^2 + \alpha_i^2 |s_i|^4\right) + \sum_{i,j} \beta_{ij} f_c(r_{ij})\, s_i \cdot s_j\right]$$

Coordinate part: use neural network

Spin part: use coefficient model

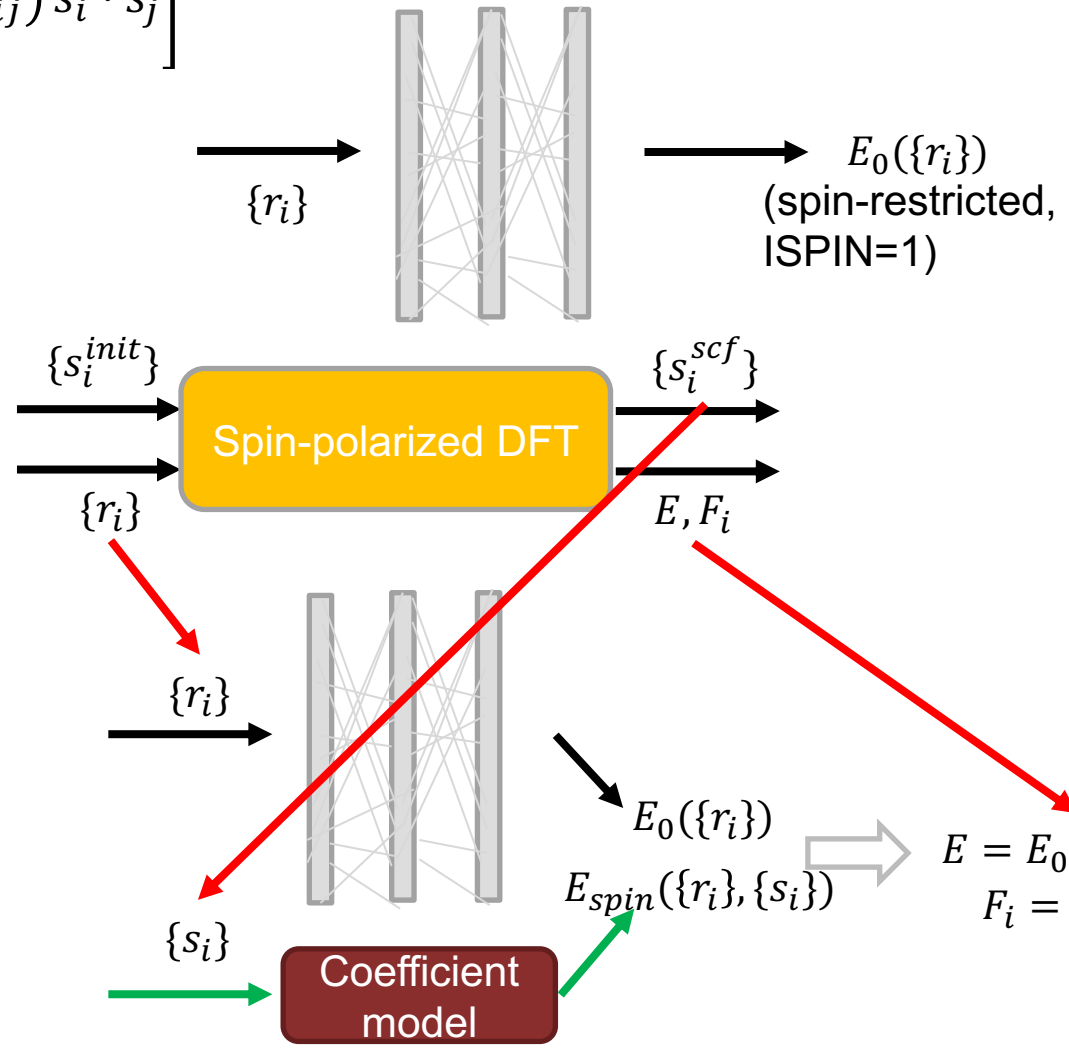

Train the two parts separately:

1. Learn spin non-polarized NN potential E_0 by the standard procedure

2. For each atomic configuration, sample different initial magnetism of know phases.

3. Linear regression on coefficients α_i^k, β_{ij} in E_{spin} by the difference $E_{DFT}(s,r) - E_0^{DFT}(r)$

4. Combine them to predict

Technical Backup:

SANNIP for Fe: Methodology testing

Training: $E_0(\{r_i\})$ converges to $\Delta E = 3$ meV/atom

Magnetism: Energy *vs* volume of different magnetic states

γ –phase

α –phase

SANNIP energy

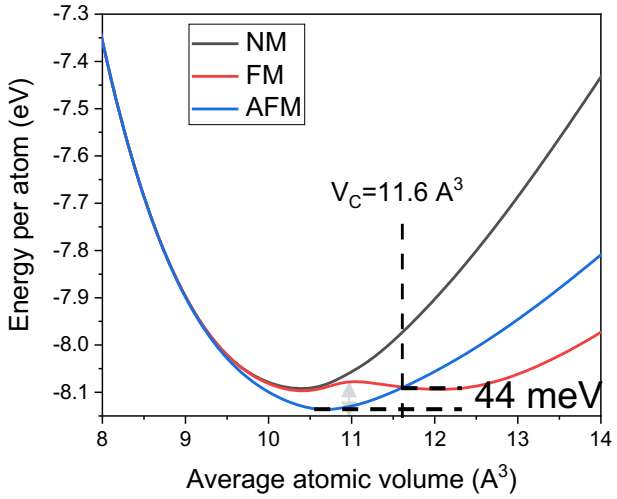

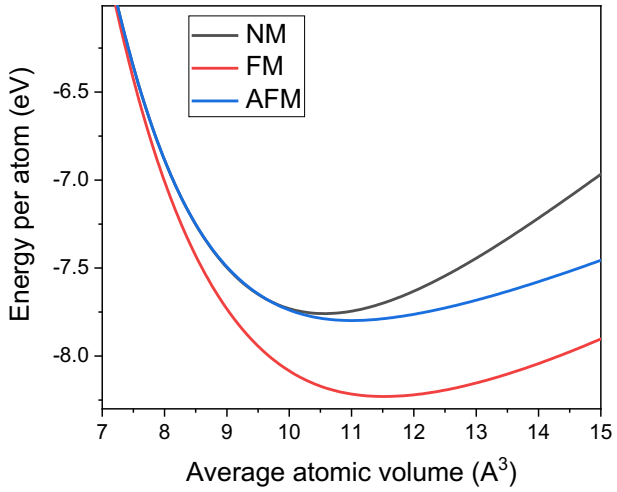

Previous DFT from literature

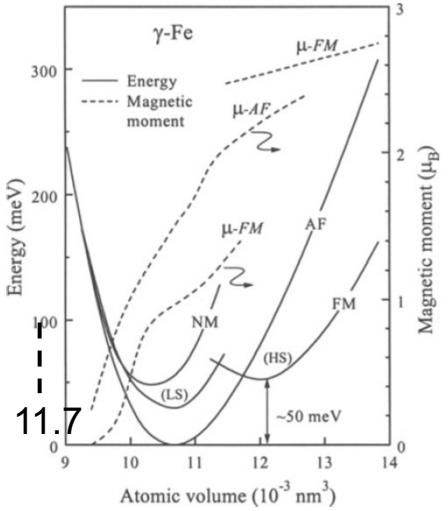

Fig. 2.19. The atomic volume dependence of the total energy and magnetic moment for the various magnetic states of γ-Fe [32].

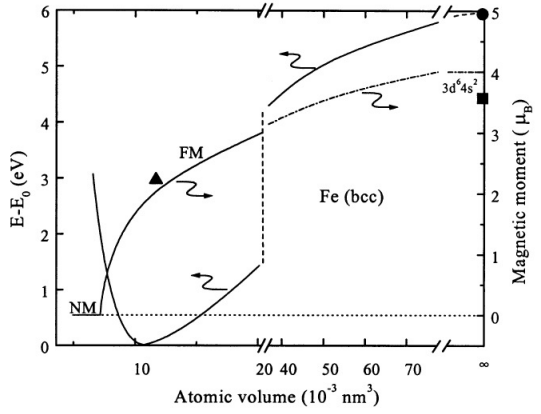

Fig. 2.12. The calculated atomic volume dependence of the total Energy E−E$_0$ (relative to the ground state) and the magnetic moment [8]. ▲ μ$_0$ (experiment). Cohesive energy for V$_a$ → ∞): ● calculated, ■ experiment (from heat of sublimation; see Tab. 3.1).

SANNIP spin

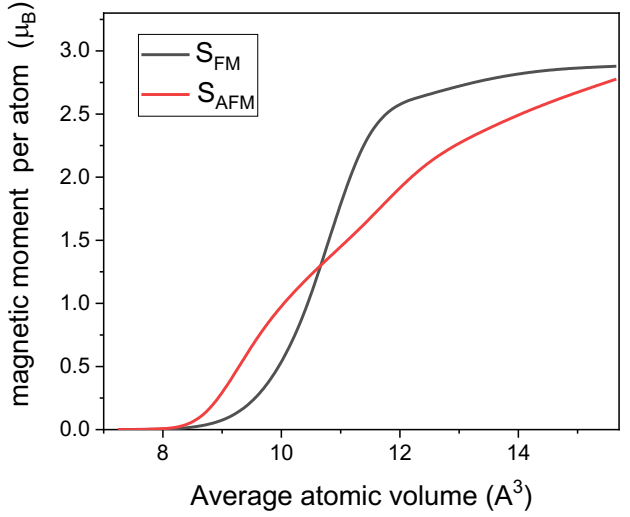

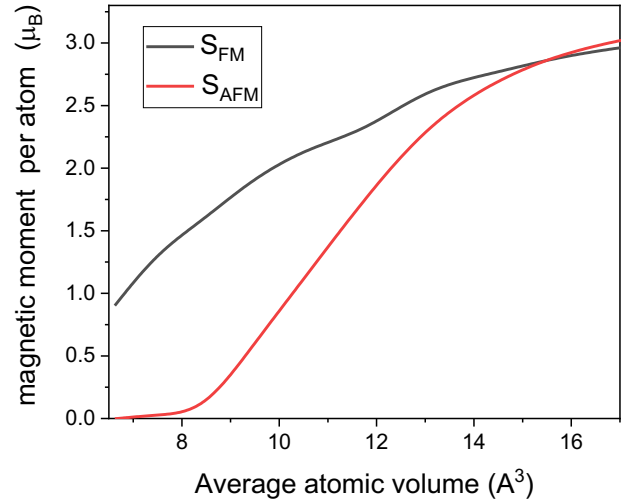

Technical Backup:

Simulation of ϵ-martensite energy in $Fe_{45}Mn_{35}Co_{10}Cr_{10}$-H

- NNIP shows that hcp phase (ϵ-martensite) has a slightly lower energy than fcc (without H)
- Checked by DFT
- DFT also shows hcp has a lower energy (without H)
- When increasing H concentration, FCC energy becomes lower.
- We examined the average intercalation energy of H: FCC octahedral site: $-3.21 \pm 0.02\ eV$
- HCP octahedral site: $-3.04 \pm 0.03\ eV$

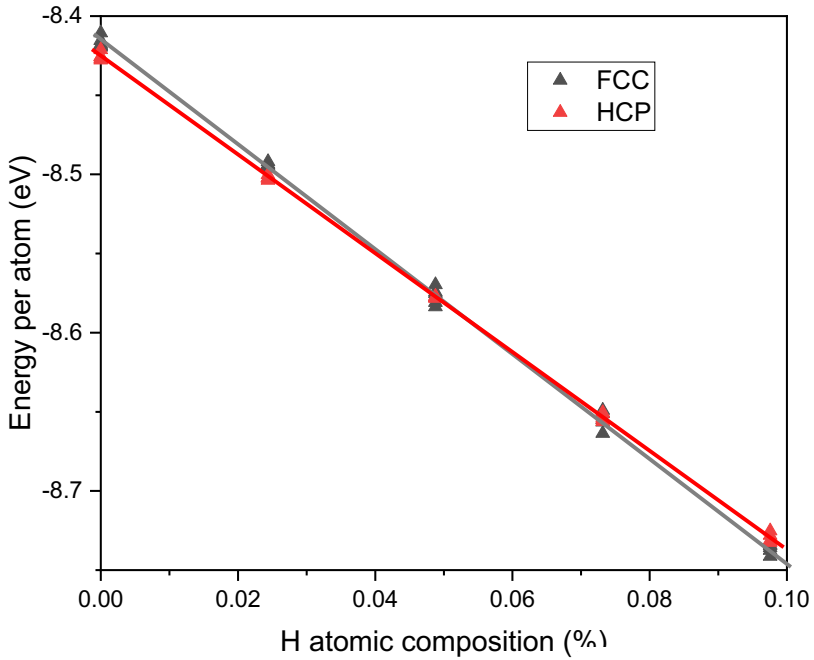

Technical Backup:

Hybrid MD-GCMC to charge hydrogen

(a)

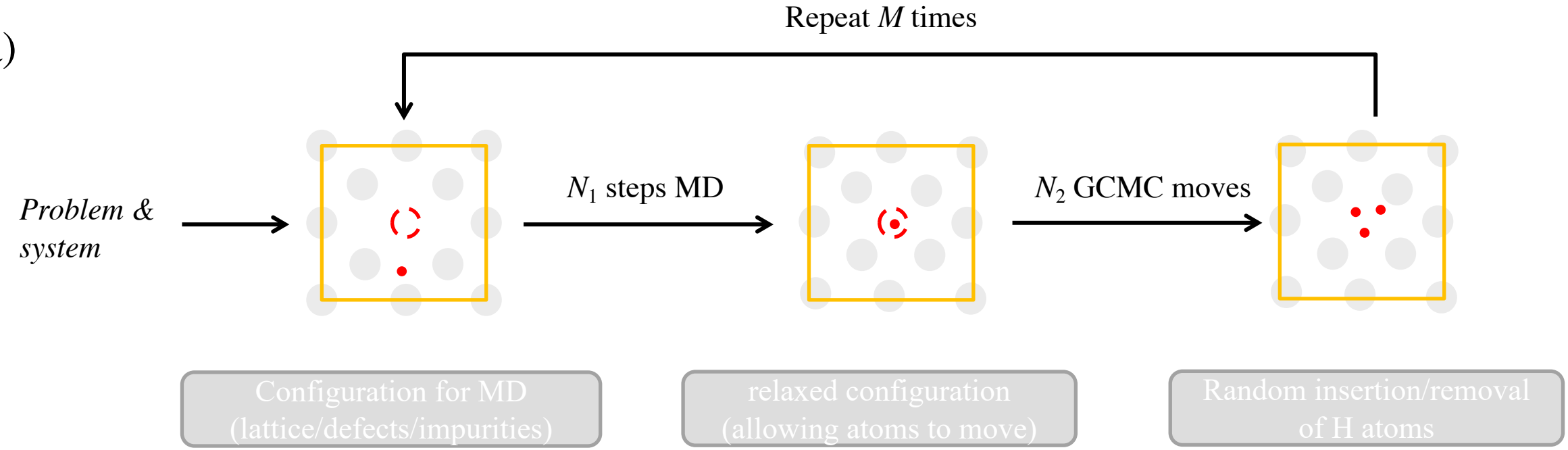

(b)

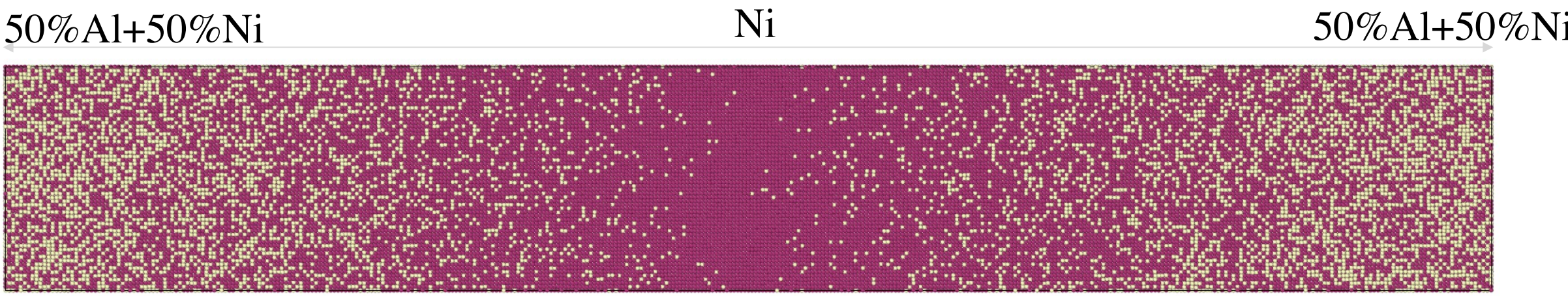

Technical Backup:

Training Data Generation for NNIP Development

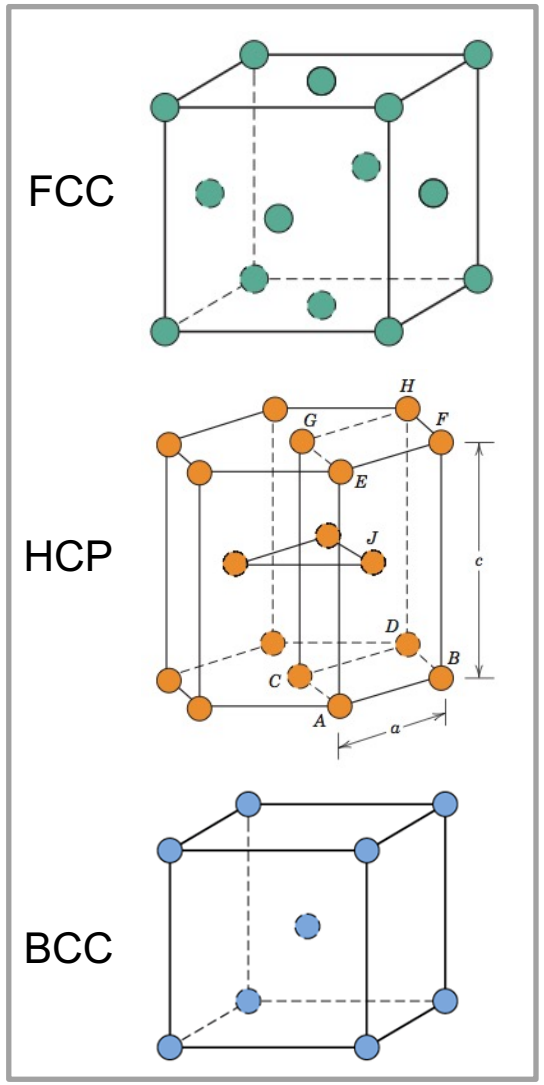

- Different replications of unit cell
- Random anisotropic scaling of supercell (-10% - 10%)
- Radom atomic displacement (stdev=0.05 A)
- Random insertion of 1 H

→ ~20,000 FCC RSS with/without H

→ ~20,000 HCP RSS with/without H

→ ~6,000 BCC RSS with/without H

# of atoms per configuration: 12 - 32

Technical Backup:
Neural Network Interatomic Potential Framework

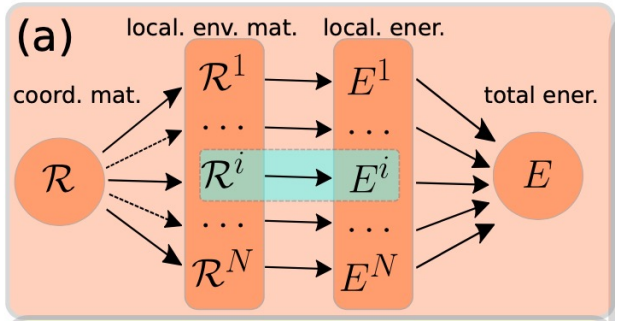

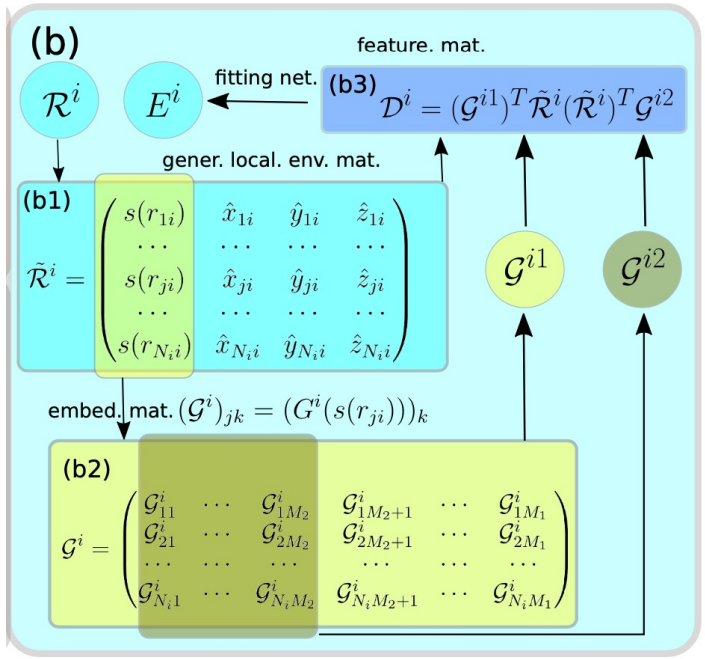

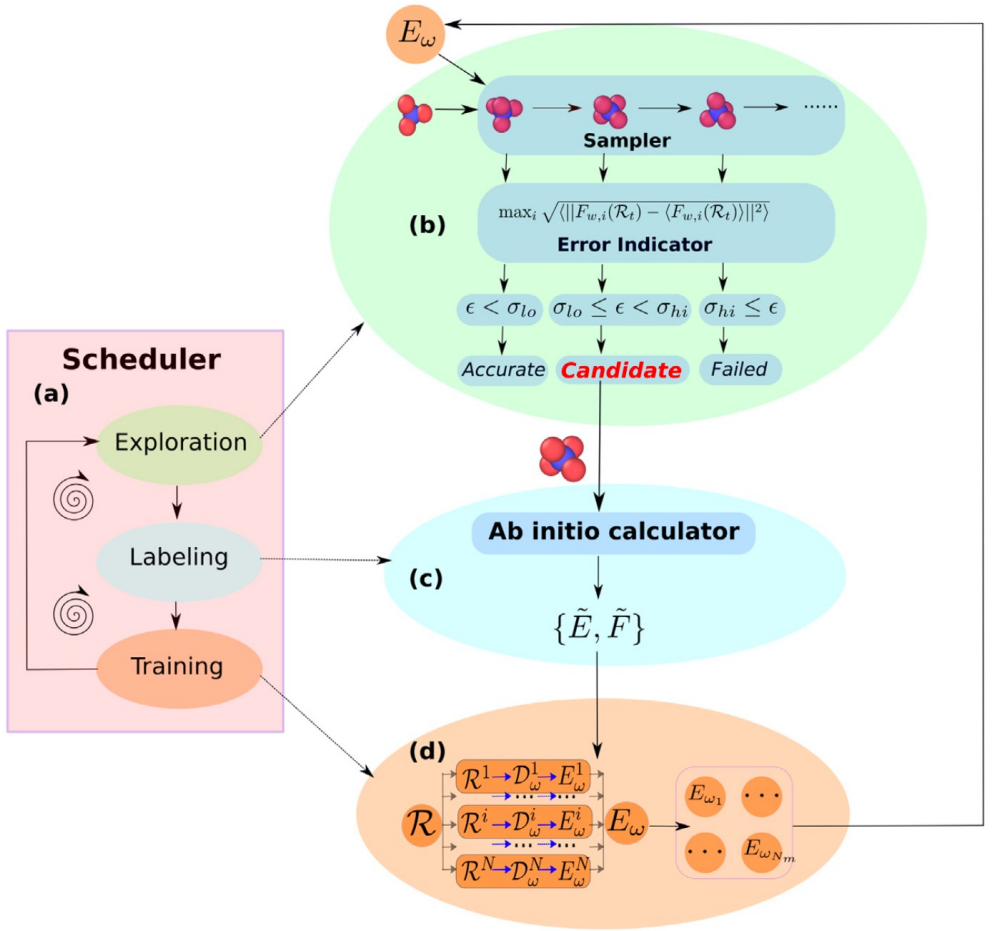

Method for correction of compliance due to substrate deflection

$$C = C_f + \frac{\sqrt{\pi}}{2E_{eff}} \frac{1}{\sqrt{A_c}} + C_{sub}$$

directly measured by using continuous stiffness measurement (CSM) as a function of contact depth h_c

Pre-calibrated (using fused silica) to C_f (constant) and $A_c = f_A(h_c)$

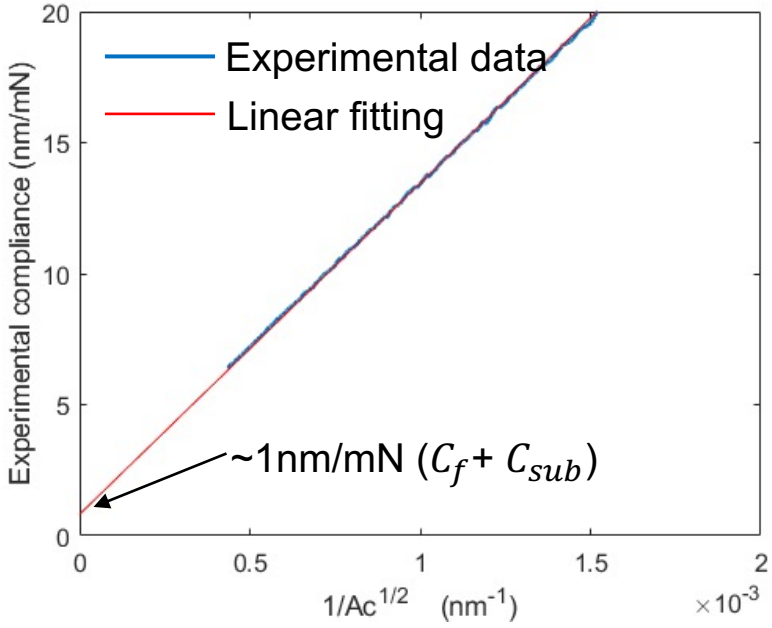

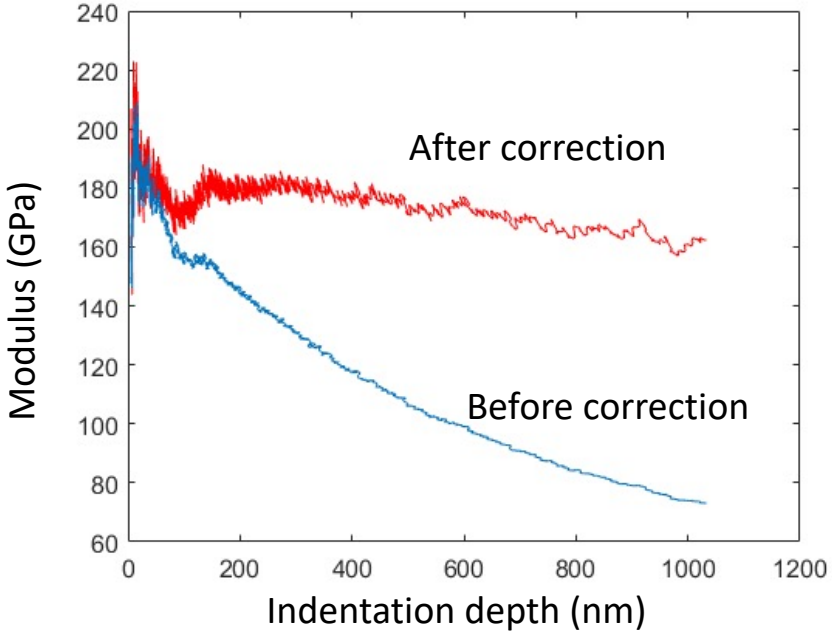

Technical Backup:

Selection of substrate for HT toughness evaluation

Quartz (Z-cut)	Fused silica	Si	Si (45° rotation)
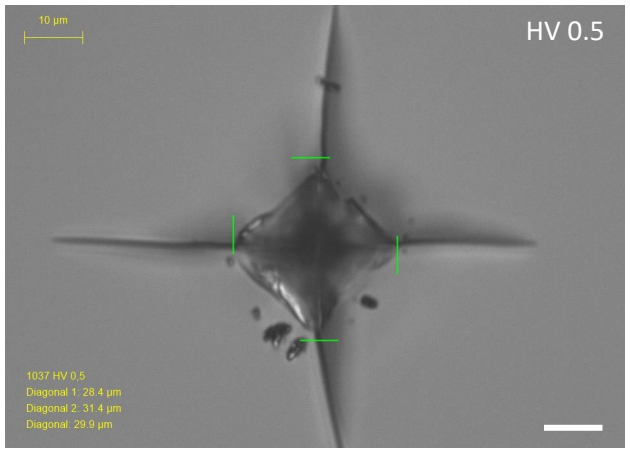	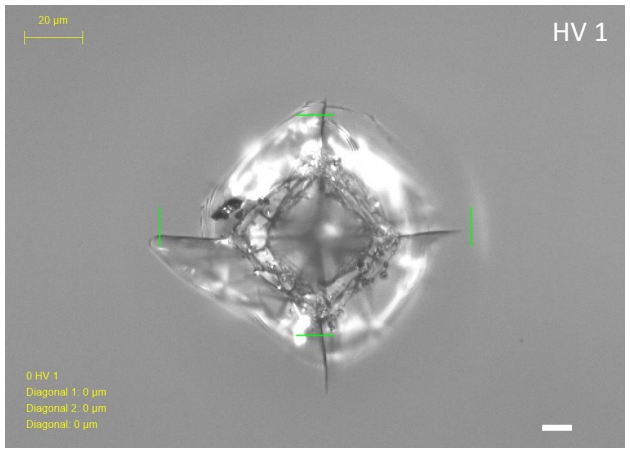	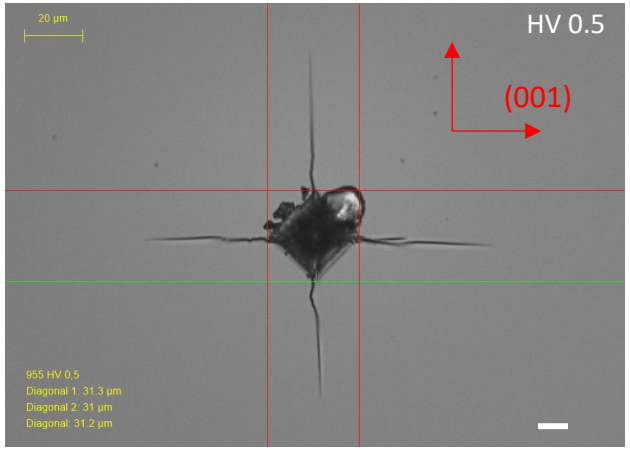	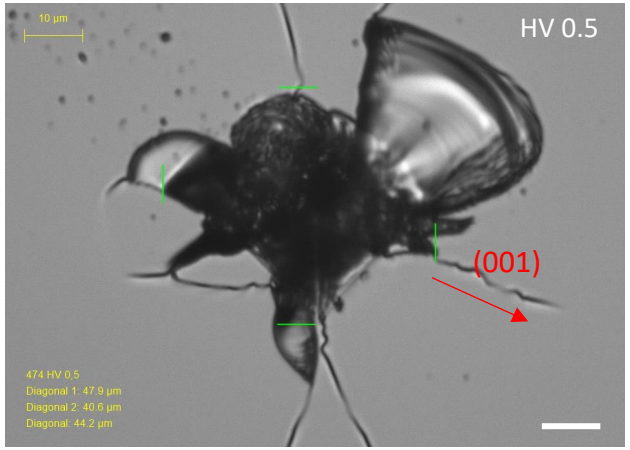
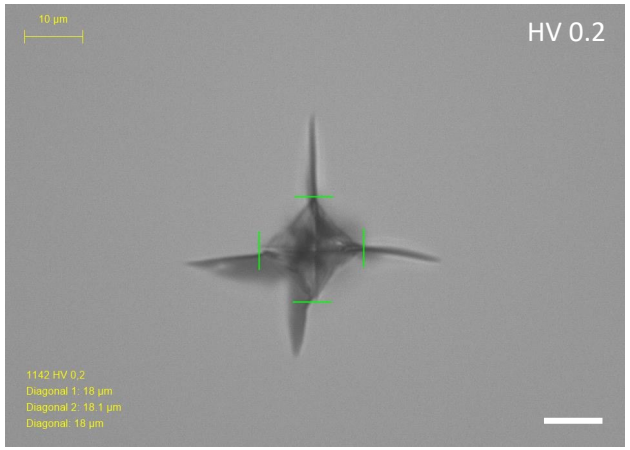	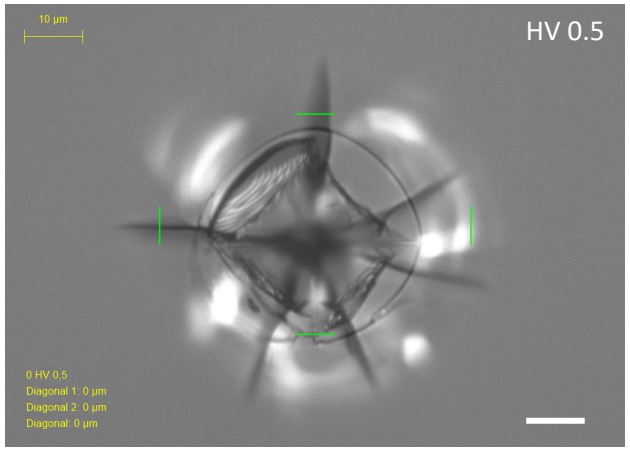	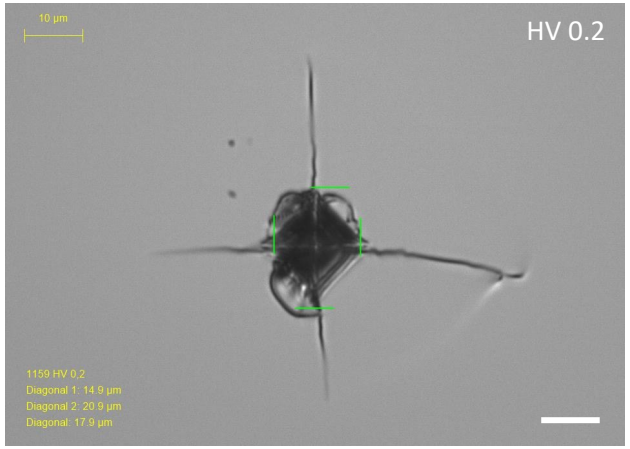	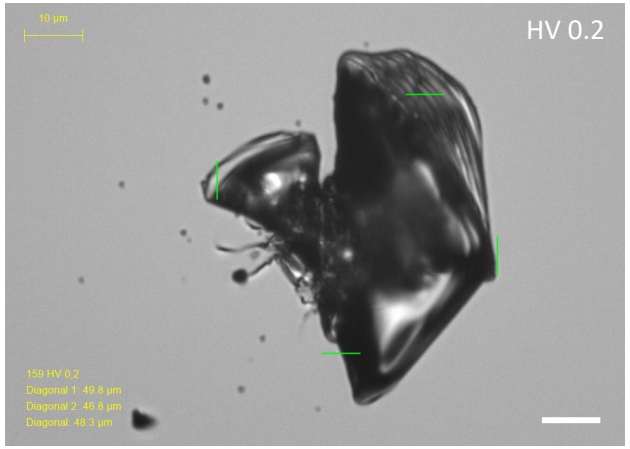

Technical Backup:

Fracture toughness and high-throughput mechanical testing

Novel Bulge Testing

High-throughput large deformations of islands with selected composition

High-precision measure of fracture toughness of selected compositions

From nanoindentation:

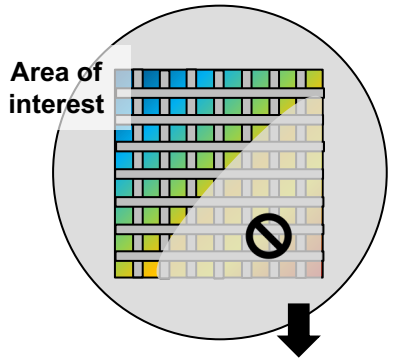

CSI more refined in area of interest:

Bulging of multiple CSI:

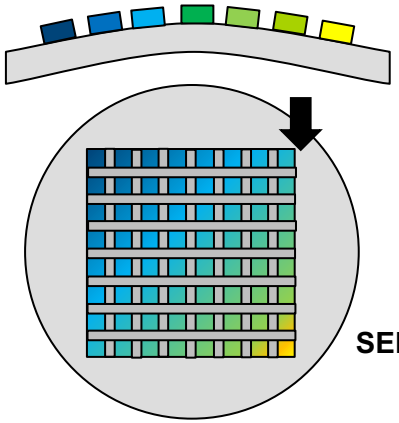

SEM imaging

For selected compositions of interest create free standing single membranes:

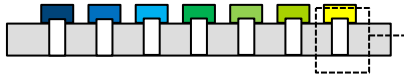

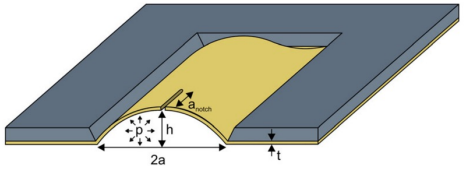

Our Co-PI J.J. Vlassak at Harvard has already established

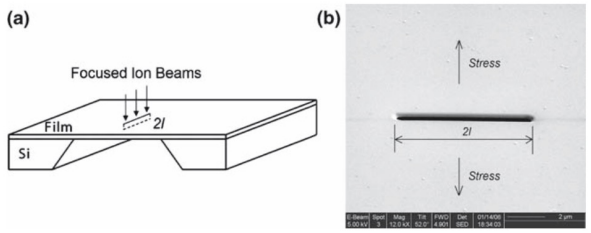

Vlassak et al. (2007) *Int J Fract*, 144:173–179

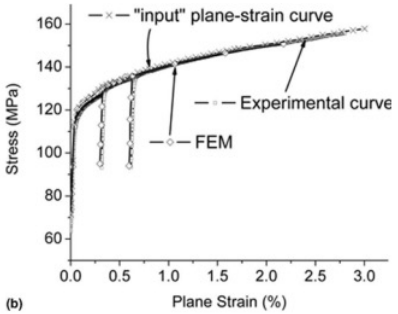

Vlassak et al. (2005) *J. Mater. Res*, 20(9) 2360

Technical Backup:
Hydrogen Mapping with 500nm resolution in SEM

2) Hydride-forming nanoparticles mapping method

- Certain transition metals form hydrides upon exposure to hydrogen
- Palladium is particularly known to be “H sponge”
- PdH_x “alloy” of Pd with metallic H, with FCC structure like Pd and two different crystallin phases:

α if $x < 0.017$

β if $x > 0.58$

x can get close to 1 with electrochemical charging as done in our tests

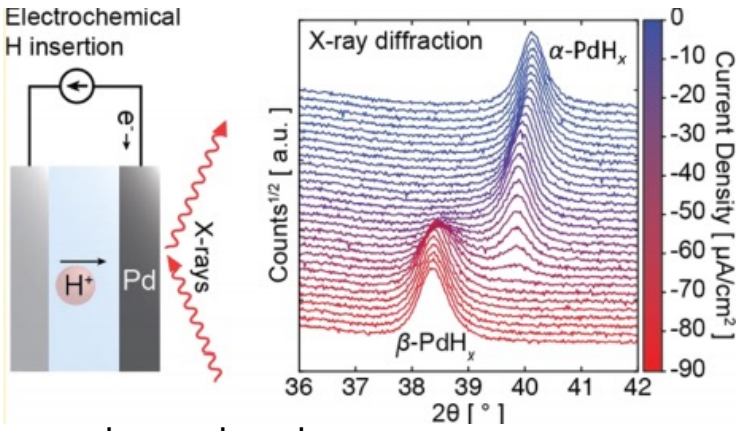

- Upon hydride formation → large change in volume

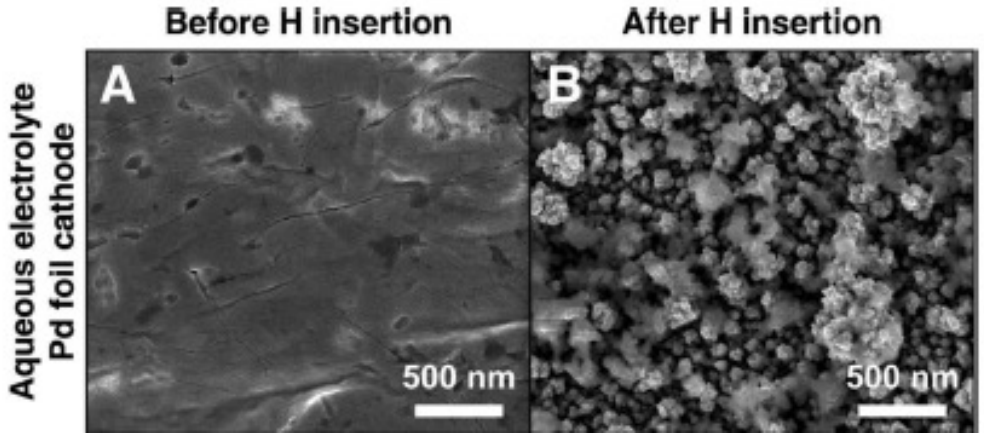

Our Hypothesis: Pd Nanoparticles (NPs) distributed on sample surface will change size as sample is H-charged

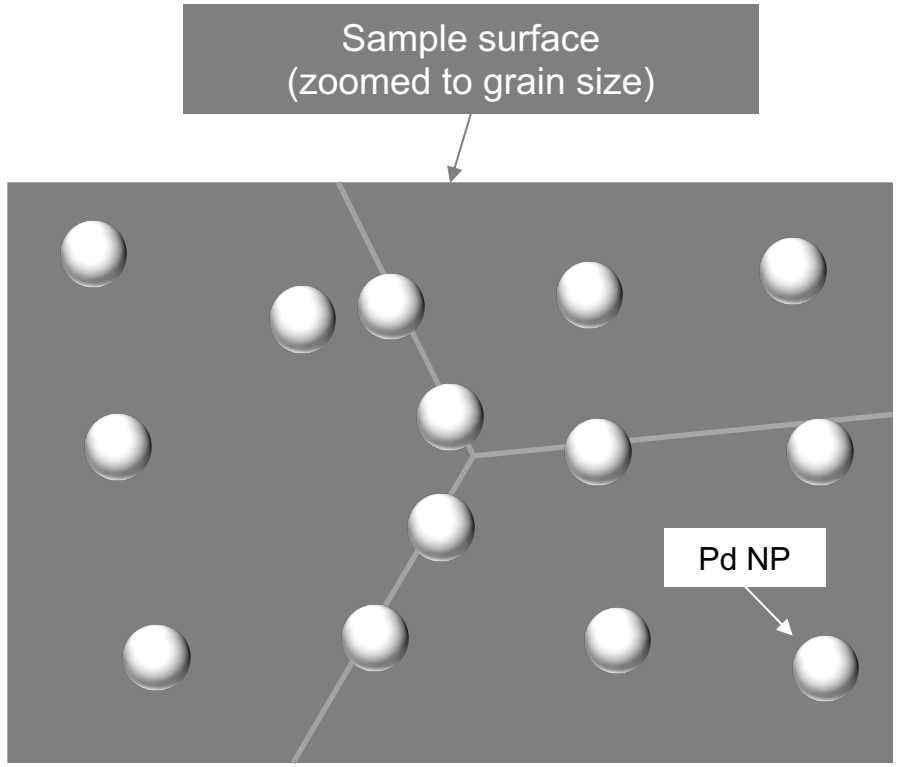

Before H-charging

Technical Backup:
Hydrogen Mapping with 500nm resolution in SEM

2) Hydride-forming nanoparticles mapping method

- Certain transition metals form hydrides upon exposure to hydrogen
- Palladium is particularly known to be “H sponge”
- PdH_x “alloy” of Pd with metallic H, with FCC structure like Pd and two different crystallin phases:

α if $x < 0.017$

β if $x > 0.58$

x can get close to 1 with electrochemical charging as done in our tests

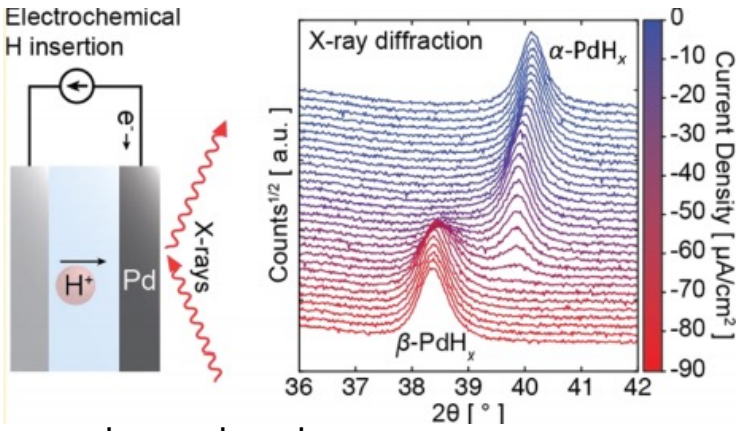

- Upon hydride formation → large change in volume

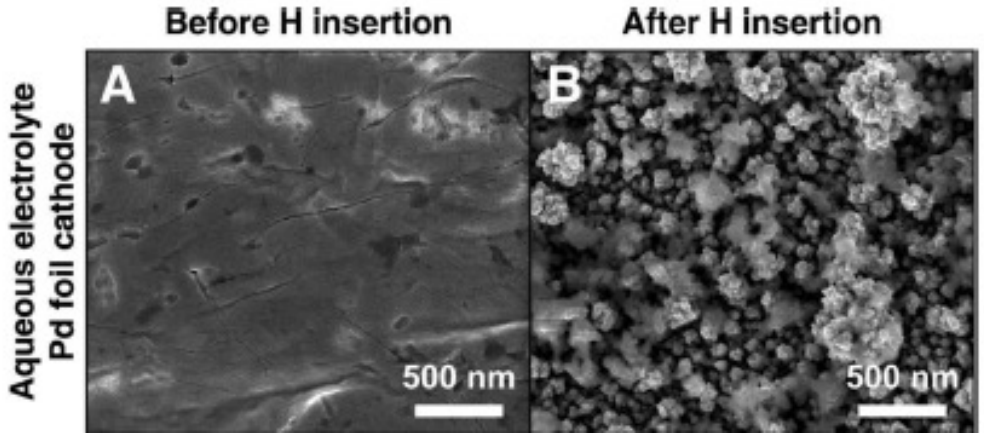

Our Hypothesis: Pd Nanoparticles (NPs) distributed on sample surface will change size as sample is H-charged

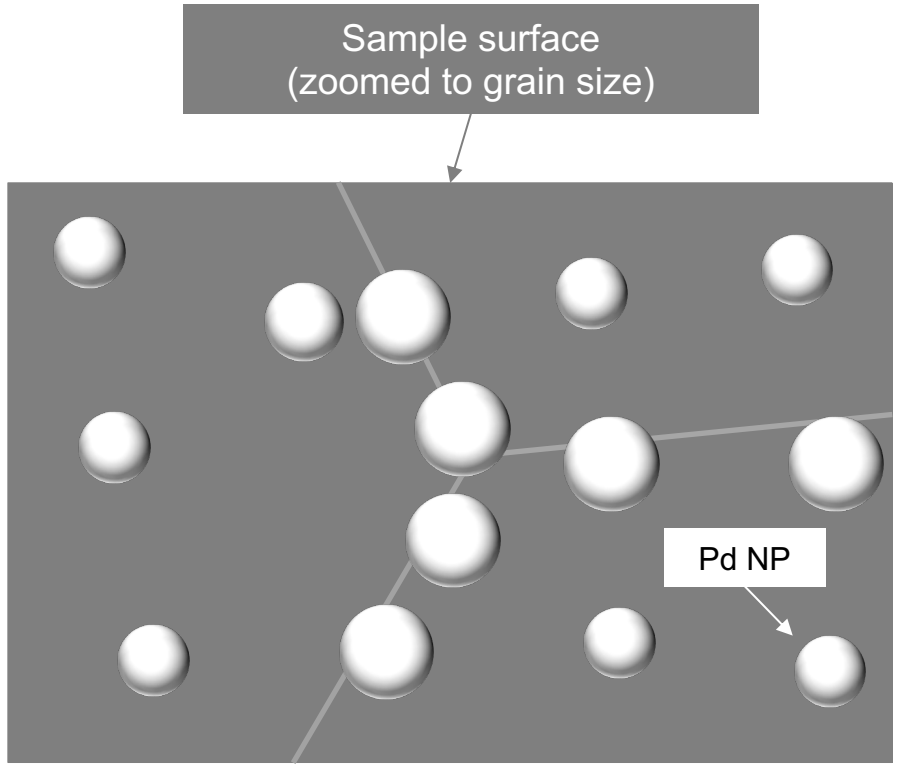

After H-charging

Technical Backup:
Hydrogen Mapping with 500nm resolution in SEM

2) Hydride-forming nanoparticles mapping method

Step 1: Pd nanoparticles deposition

PdH_x as a very "rough" surface

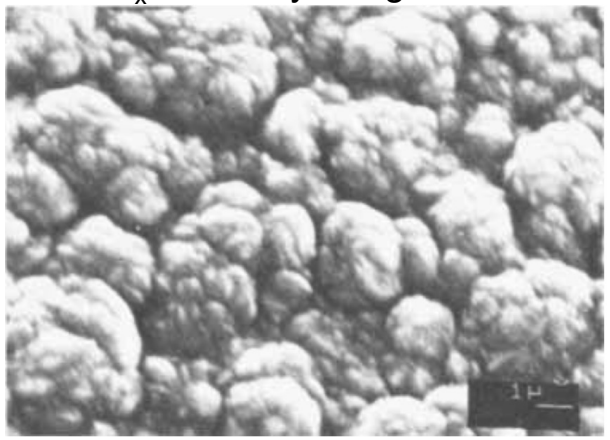

Raub (1982) *Platinum Metals Rev.*, 26, (4), 158-166

Pd can deposit directly as PdH_x which would make our particles insensitive to more hydrogen.

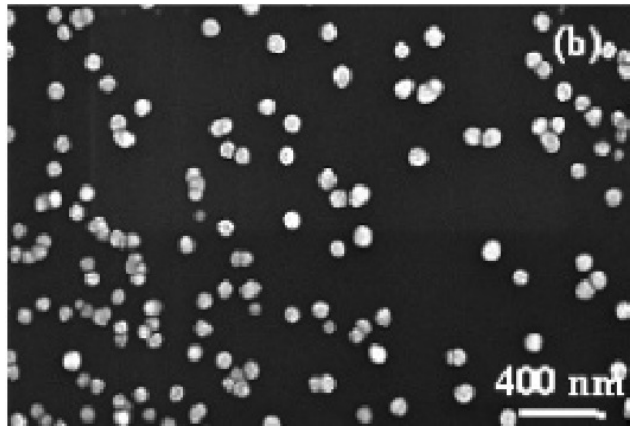

Joshi et al. (2008) *J. Phys. Chem. C*, 112, 1857-1864

It is possible to deposit pure, spherical Pd nanoparticles by tuning:

- Electrolyte
- Deposition method/conditions

Electro-deposition

- **5g/L $PdCl_2$ in distilled water + NH_4OH 30%**
- **50s** deposition at -5 A/m^2

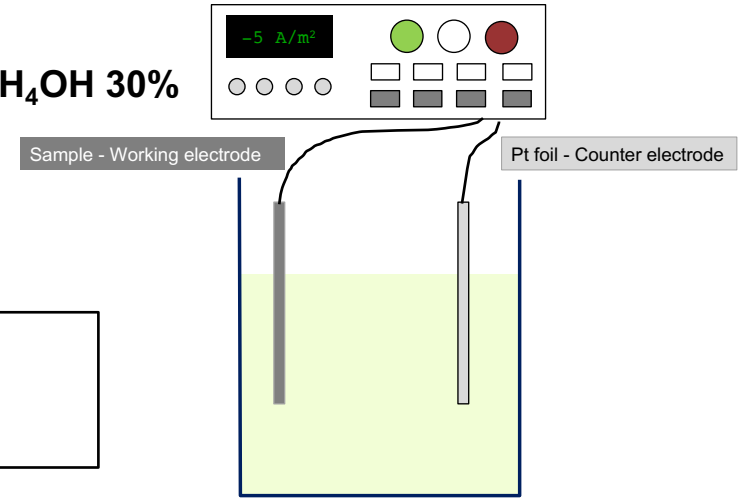

- Correct size (controllable with deposition time)
- Homogeneous distribution